Multidisciplinary Design Optimization of an Electric Race Car

Lucas Anthony Crea

Department of Mechanical Engineering

McGill University, Montreal

December 2021

A thesis submitted to McGill University in partial fulfillment of the requirements of the degree of Master of Science.

Acknowledgments

I would like to thank my supervisor, Prof. Michael Kokkolaras, for his support and guidance all throughout this degree.

I would also like to acknowledge members of McGill Formula Electric for their help in making this work possible. A big thank you to Benjamin Munt, David Green, Ali Al-Taher, Thomas Yin, Matteo Barbieri and Sakib Hasan who provided valuable insights on vehicle subsystems, made computational resources available and shared existing models.

Finally, a special thank you to my fiance, family and friends for their never ending support.

Table of Contents

Table of Contents ii

List of Figures iv

List of Tables vi

1 Introduction 1

2 Review of the literature 4

2.1 MDO in the automotive industry 4

2.2 Electric vehicle optimization 7

3 Modeling 10

3.1 Competition model 10

3.1.1 Acceleration scoring 12

3.1.2 Skid-pad scoring 13

3.1.3 Autocross scoring 14

3.1.4 Endurance scoring 15

3.1.5 Efficiency scoring 16

3.2 Vehicle models 18

3.3 Subsystem models 21

3.3.1 External aerodynamics 22

3.3.2 Accumulator . . . 23
3.3.3 Gear train . . . 25
3.4 Lap simulation . . . 27
3.4.1 Acceleration . . . 30
3.4.2 Skid-pad . . . 30
3.4.3 Autocross & endurance . . . 30

4 Multidisciplinary Design Optimization Framework 34
4.1 Vehicle-level optimization . . . 35
4.2 Subsystem-level optimization . . . 37
4.2.1 Accumulator . . . 37
4.2.2 Gear train . . . 40

5 Numerical Results 43
5.1 Individual event optimization . . . 45
5.1.1 Optimizing for acceleration . . . 47
5.1.2 Optimizing for skid-pad . . . 49
5.1.3 Optimizing for autocross . . . 49
5.1.4 Optimizing for endurance . . . 50
5.1.5 Optimizing for efficiency . . . 52
5.2 Optimizing for all events . . . 54
5.3 Optimizing for all events with relaxed constraints . . . 55

6 Conclusion 60
6.1 Outlook . . . 61

List of Figures

3.1 Scoring relative to t_{min}. 11

3.2 Skidpad track [1]. 13

3.3 Autocross track layout. 14

3.4 Endurance track layout. 15

3.5 Efficiency points vs average CO_2 and lap time. 17

3.6 Hoosier 18.0x6.0 LCO 7in tire model. 19

3.7 Simplified tire model. 19

3.8 AMK motor characteristics at 600V. 20

3.9 Simplified vehicle CAD model. 22

3.10 External aerodynamics velocity streamlines. 23

3.11 Example CAD model of module and battery pack. 24

3.12 Annotated gear train with ring gear as output. 26

3.13 Interrelationship between the MDO and lap simulation processes. 27

3.14 Autocross lap simulation flowchart. 31

3.15 Autocross speed profile at different lap simulation steps. 32

4.1 XDSM of optimization and analysis framework. 35

5.1 Speed differences of the optimal vehicle for the acceleration optimization study. 48

5.2 Speed differences of the optimal vehicle for the autocross optimization study. 50

5.3 Speed differences of the optimal vehicle for the endurance optimization study. 52

5.4 Speed differences of the optimal vehicle for the efficiency optimization study. 54

List of Tables

3.1 Summary of vehicle parameters. 21

5.1 Baseline vehicle. 43

5.2 Baseline front and rear gear train designs. 44

5.3 Baseline accumulator design. 44

5.4 Feasible accumulator designs at 600V. 45

5.5 Individual event optimization results with best results shown in blue. 46

5.6 Optimal vehicle variables for each individual event optimization study. . . . 46

5.7 Optimal gear train variables for each individual event optimization study. . . 46

5.8 Lap simulation analysis for each individual event optimization study. 47

5.9 Energy related lap simulation results for the endurance optimization study. . 51

5.10 Energy related lap simulation results for the efficiency optimization study. . 53

5.11 All event optimization results with best result shown in blue. 55

5.12 Optimal vehicle variables for the overall competition optimization study. . . 55

5.13 Front and rear gear train designs for the overall competition optimization study. 55

5.14 Accumulator designs with relaxed constraints. 57

5.15 Top 10 all event optimization results with relaxed battery constraints. 58

5.16 Optimal vehicle variables for the top 10 overall competition optimization studies with relaxed constraints. 59

Nomenclature

Acronyms

AoA Angle of attack

AOF Aggregate objective function

ATC Analytical target cascading

CFD Computational fluid dynamics

CoG Center of gravity

CoP Center of pressure

CO Collaborative optimization

DOF Degree of freedom

EV Electric vehicle

FSAE Formula Society of Automotive Engineering

IDF Individual discipline feasible

IWD Individual wheel drive

K&C Kinematic and compliance

MADS Mesh adaptive direct search

MDO Multidisciplinary design optimization

MFE McGill Formula Electric

R&H Ride and handling

VDC DC voltage

XDSM Extended design structure matrix

Symbols

α_{F3} Front element 3 angle of attack

α_{R2} Rear element 2 angle of attack

α_{R3} Rear element 3 angle of attack

$\dot{\theta}$ Angular velocity

η Efficiency factor

τ Torque

$\mathbf{x}_{\text{Acc}}$ Accumulator variables

$\mathbf{x}_{\text{Gear}}$ Gear variables

$\mathbf{x}_{\text{veh}}$ Vehicle variables

$\widetilde{\mathbf{x}}_{\text{veh}}$ Fixed vehicle and subsystem design

C_{Cell} Cell capacity

CO_2 Carbon dioxide

D_{CB_i} Cumulative bending damage on gear i

D_{CS_i} Cumulative surface damage on stage i

d_{o} Outer diameter of gear train

DP_i Stage i diametral pitch

ds Track segment length

E_{A} Accumulator energy

E_{d} Volumetric energy density

E_{T} Energy target

F Force

F_{W_i} Stage i face width

GR Gear train gear ratio

$GR_{\mathrm{F_T}}$ Front gear ratio target

$GR_{\mathrm{R_T}}$ Rear gear ratio target

GR_{T} Gear ratio target

H_{A} Accumulator height

$I_{\mathrm{charge_{cell}}}$ Cell peak charge current

$I_{\mathrm{charge_{max}}}$ Peak charge current

$I_{\mathrm{discharge_{cell}}}$ Cell peak discharge current

$I_{\mathrm{discharge_{max}}}$ Peak discharge current

L_{A} Accumulator length

m_{A} Accumulator mass

m_{gear} Gear train mass

m_{veh} Vehicle mass

$n_{\text{C}_{\text{ML}}}$ Number of parallel cell bundles per module length-wise

$n_{\text{C}_{\text{MW}}}$ Number of parallel cell bundles per module width-wise

$n_{\text{C}_{\text{P}}}$ Number of cells in parallel

$n_{\text{C}_{\text{S}}}$ Number of parallel cell bundles connected in series

n_{ML} Number of modules length-wise

n_{MW} Number of modules width-wise

n_{T_i} Number of teeth on gear i

O_{RG} Output ring gear

P Power

$P_{\text{charge}_{\text{min}}}$ Minimum charge power

P_{charge} Accumulator maximum charge power

$P_{\text{discharge}}$ Accumulator maximum discharge power

P_{limit} Vehicle power limit

r Radius

s Track segment

SV_{E} Energy surplus and slack variable

SV_{G} Gear ratio surplus and slack variable

SV_{V} Voltage surplus and slack variable

t Time

T_{C} Cell type

V Voltage

v Velocity

V_{A} Accumulator Voltage

V_{cell} Cell voltage

V_{T} Voltage target

W_{A} Accumulator width

Abstract

The design and optimization of electric race cars is increasingly relevant. The complexity and flexibility of electrified powertrains poses challenges and offers opportunities for design optimization. To this end, this work presents the multidisciplinary design optimization (MDO) framework developed to optimize a four individual wheel drive (IWD) electric vehicle destined to compete in Formula Society of Automotive Engineering competitions. Each of the different events that make up these competitions are taken into account in the optimization problem formulation. The considered disciplines include the external aerodynamics, the accumulator and the front and rear gear trains. This work first describes the models used and developed to predict the behaviour of these subsystems. It then describes a lap simulation method, based on quasi-steady-state approaches, specifically created to evaluate the designs produced by the MDO framework. The integration of the various models used in the framework is subsequently presented.

Several optimization studies are conducted using the developed framework. The performance and effectiveness of the proposed methodology is first evaluated via the optimization of the vehicle for each event in the competition. The obtained results demonstrate clearly that the MDO environment is capable of yielding improved designs. The results also highlighted the need to optimize certain parts of the vehicle that can be changed in-between events and that the developed framework would be capable of achieving it. The case study utilizing a single objective function that includes all events also yields promising results. Although this new design is not significantly better, the fact that it improves a very mature

one confirms the usefulness of such an MDO environment during early design stages.

Résumé

La conception et l'optimisation des voitures de course électriques sont de plus en plus pertinentes. La complexité et la flexibilité des groupes motopropulseurs électrifiés posent des défis et offrent des opportunités d'optimisation. À cette fin, ce travail présente le cadre d'optimisation de la conception multidisciplinaire (MDO) développé pour optimiser un véhicule électrique à quatre roues motrices individuelles (IWD) destiné à participer aux compétitions de la Formula Society of Automotive Engineering. Chacun des différents événements qui composent ces compétitions est pris en compte dans la formulation du problème d'optimisation. Les disciplines considérées incluent l'aérodynamique externe, l'accumulateur et les trains d'engrenages avant et arrière. Ce travail décrit d'abord les modèles utilisés et développés pour prédire le comportement de ces sous-systèmes. Il décrit ensuite une méthode de simulation de tours, basée sur des approches quasi stationnaires, spécifiquement créée pour évaluer les conceptions produites par le cadre MDO. L'intégration des différents modèles utilisés dans le cadre est ensuite présentée.

Plusieurs études d'optimisation sont menées en utilisant le cadre développé. La performance et l'efficacité de la méthodologie proposée sont d'abord évaluées via l'optimisation du véhicule pour chaque épreuve de la compétition. Les résultats obtenus démontrent clairement que l'environnement MDO est capable de produire des concepts améliorés. Les résultats ont également mis en évidence la nécessité d'optimiser certaines parties du véhicule qui peuvent être modifiées entre les événements et que le cadre développé serait capable d'y parvenir. L'étude de cas utilisant une fonction objectif unique qui inclut tous les événements

donne également des résultats prometteurs. Bien que cette nouvelle conception ne soit pas significativement meilleure, le fait qu'elle améliore un concept très mature confirme l'utilité d'un tel environnement MDO lors des premières étapes de conception.

Chapter 1

Introduction

Designing racing cars destined to compete in motorsport championships is a laborious practice in which engineers engage in a multidisciplinary search for the highest performing vehicle. The difficulty of this exercise stems from the conflicting nature and the complex interactions of the numerous engineering disciplines required to design a vehicle which ultimately influences the dynamic capabilities of the car in question.

In various motorsport championships, the winning car, being the highest performer, is either the one that finishes a race first or the one that accumulated the most amount of points across multiple races. In such championships, the objective of the optimization problem can be said to be the minimization of lap-times. However, considering that multi-event championships are usually held in vastly different purpose-built circuits, optimization exercises may provide better results by evaluating the performance of the race car across the multiple tracks. This is due to the fact that the performance of a vehicle designed for a specific track may not necessarily translate on another.

Furthermore, the recent global push for the electrification of transportation has made its way into the world of motorsports. Electric vehicles (EVs) bring with them a great deal of new disciplines and design variables such as: the number of electric motors, their placement (e.g., in-wheel vs. on-board motors) and control (e.g., torque vectoring), as well as battery

design and energy management (e.g., regenerative braking) [2]. As such, the new variables and control opportunities that an electrified powertrain provide could greatly increase the complexity of a design optimization study.

Given the above, the need for multidisciplinary design optimization (MDO) in the conceptual design stage of the development of electric race car is evident. Such a strategy could not only help teams understand the complex interactions between subsystems early on, but could also accelerate the conceptual design process. As such, the main objective of this work is the development of an optimization framework for electric race cars that not only examines their unique engineering challenges but also considers multiple tracks. A perfect practical candidate for such work is the design and optimization of the university's four individual wheel drive electric race car which competes in Formula Society of Automotive Engineering (FSAE) Electric championships. These competitions not only evaluate the electric car's lap times but also it's efficiency across different circuits.

To ensure that the development of this framework is usable and expandable by the McGill Formula Electric (MFE), the university's FSAE team, the following requirements were imposed:

- The framework should be implemented in MATLAB such that it would be compatible with MFE's current workflow.
- The framework must have a distributed architecture (optimization problem partitioned into subproblems [3]) to match the organization management structure.
- The framework must allow for users to optimize the subsystems (i.e., subproblems) independently, if desired.

Considering the outcome of this work will be a first iteration of a MDO environment for MFE, the scope of this project will be limited to three subsystems of the vehicle: (1) battery pack, (2) gear trains for both front and rear axles and (3) the external aerodynamic setup of the vehicle. The models for the battery pack and aerodynamics were purposely built for

this work while the gear train model was developed and provided by the university's FSAE team. To evaluate the performance of the vehicle, a steady-state two-track lap simulation methodology was developed.

This thesis is organized into six chapters. The second chapter is an overview of the literature surrounding MDO in the automotive industry and electric vehicle optimization. The third chapter will cover the models developed and used by the MDO framework. The fourth chapter will detail the optimization problems being solved at the system and subsystem levels. In the fifth chapter, an overview and discussion of the results is presented. In the sixth and final chapter, a conclusion summarizing the research is given and suggestions to improve the developed framework are proposed.

Chapter 2

Review of the literature

2.1 MDO in the automotive industry

Over the last 25 years, researchers have been making advancements in the field of MDO to address the issues associated to the multidisciplinary nature of engineering systems. In particular, the main motivation has been to enable concurrent design by the various engineering teams within an organization [4, 5]. Despite the fact that both the aerospace and automotive industries tackle engineering issues of similar complexities, most of the research in large scale MDO has been linked to the aerospace industry [4]. As the papers showcased below illustrate, the research in the automotive industry tends to focuses on smaller scale MDO frameworks.

In [5], Kim et al. demonstrate the use of analytical target cascading (ATC) in automotive engineering via a ride and handling optimization problem. The subsystems, which are the "higher-level" systems in the framework, were the the vehicle ride and handling (R&H) targets. The subsystem components, or "lower-level" systems, were the front and rear suspension, and vertical and cornering stiffness. In a similar fashion, in [6], Kang et al. in partnership with Hyundai Motor Company, show the implementation of ATC for two distinct problems, the suspension design of a heavy-duty truck and the body structure design

of a bus. The goal of the first problem was to design the suspension characteristic of the three suspensions of the truck such that the axle weights are limited to 10 000kg. The second problem's objective was to minimize the mass body weight while keeping the structural stiffness of the assemblies by optimizing the beam cross sections. Although [5] and [6] are case studies for MDO in the automotive industry, they lack a holistic vehicle perspective.

Kang et al. [7] also explored the use of an aggregate objective function (AOF) (i.e., using weighted sums of competing objectives of an multi-objective problem) to solve MDO problems. In doing so, they solve an automotive MDO problem using ATC. The example problem used was the suspension design for commercial vans which considers ride and handling. R&H is quantitatively represented through three objectives/problems: ride comfort, controllability and stability. An interesting aspect of this work is that it uses both the hierarchical and non-hierarchical formulations of ATC to solve the problem. Relating all three R&H objectives is done via the non-hierarchical form of ATC. The multi-objective decomposition of the problem allows for each of these objectives to be solved for individually. In fact, each of the individual ride and handling problems were further decomposed into a bi-level problem and using the standard hierarchical form of ATC. In more detail, at the vehicle level, the parameters of the kinematic and compliance (K&C) curves are pushed as the system level targets. At the system level, the suspension design variables are found such that its resulting K&C curves match these target curves. Finally, these suspension design variables are then shared in the non-hierarchical structure amongst all the suspension objectives to solve the AOF. Despite the fact that [7] is simply focused on a suspension design, the use of AOF is quite interesting and could certainly be very applicable to solve large scale automotive problems.

In [8], Muñoz et al. used *The Open Racing Car Simulator* (TORCS), an open-source vehicle simulator with a comprehensive physics model, to optimize the setup of a vehicle over three completely different and unrelated tracks (i.e., the optimization problem is repeated for each track). This vehicle had 22 variables relating to the gearbox ratios, front and rear wing

angles, brake system, front and rear anti-roll bar, and suspension geometry. The objective was to find the best setup that results in the longest distance covered in a given time; the authors used evolutionary algorithms to solve the problem. In [9], Köle et al. build on the work done in [8] by exploring the use of hyper-heuristic algorithms to solve the problem detailed above. Unfortunately, the works presented by Muñoz et al. and Köle et al. have the same three shortcomings: they employ monolithic optimization methods which prevent concurrent design, the scope of the individual optimization problems is limited to a single track and does not look for the overall optimal car across all tracks, and the optimal control problem associated with finding the quickest way around a track is not considered.

McAllister et al. [10], showcased the use of the *Collaborative Optimization* (CO) distributed MDO framework to optimize a simple race car that goes around a skidpad. The three design variables evaluated where the longitudinal weight distribution, the center of pressure's (CoP) longitudinal location and the roll stiffness distribution. In order to distribute the optimization work, the weight and roll stiffness distributions where handled by one local optimizer and the aerodynamic distribution by another. The actual vehicle characteristics, such as mass, dimension and aerodynamic coefficients, were parameters alongside the radius of the skid-pad. The vehicle dynamics were modelled via a bicycle model. The powertrain of the vehicle was not considered as it was not necessary for the purpose of the study. The authors were only interested in finding the maximum constant speed the vehicle can go around the skid-pad. Due to the lack of depth of the optimization, [10] can only be labelled as a very early exploration of distributed MDO methods.

Overall, the state-of-the-art for MDO in automotive engineering is fairly dated and does not truly provide case-studies for larger scale problems. The few papers that attempt to provide a whole vehicle perspective are not relevant for industry use because they either use a monolithic or lack complexity.

2.2 Electric vehicle optimization

As mentioned previously, the technology found in EVs bring with them a broad array of new design variables [2]. In particular, the use of electric motors can vastly change the traditional powertrain designs. Due to the characteristic torque-speed curves of electric motors, EVs typically have simple transmissions as the need for additional gears, often found in internal combustion vehicles to stay in an optimal torque band, is removed. Furthermore, electric motors allow for different multi-motor configurations: four on-board motors, one front and two rear on-board motors, two rear in-wheel motors, etc. Depending on the motor configuration selected, the need of differentials could be removed and transmissions could be further simplified. In addition, the use of multi-motor powertrains could allow for torque vectoring as well as for different motors and gear ratios to be used for the front and rear wheels. That being said, it is fairly evident that the flexibility of electric motors add quite a bit of design complexity from both a controls and vehicle dynamics perspective. On the battery front, the power density is dramatically lower than that of gasoline [11]. As such, great care must be taken in the battery design, in particular for ones destined to be used in an electric race car, as unnecessary weight will reduce the vehicle performance. Moreover, energy recovery systems should be examined, such as regenerative braking, to improve the vehicle's efficiency. All things considered, the existing literature on the optimization of vehicles seldom take into account the new challenges that EVs bring.

In [12], Yu et al. consider the optimal design of a powertrain of a 2-individual wheel drive (2-IWD) electric race car. To achieve this, they optimize the torque-speed curve of the electric motor by selecting the base speed and constant power speed ratio of the two motors, which are assumed to be identical, while keeping the maximum power of the motors as a fixed parameter. Further, they also consider the gear ratio and the front-rear braking bias as optimization variable. The authors created a mass model for both the electric motor and gearbox to take into account the effects of the design variables on the vehicle dynamics. It is important to note that they do not account for the center of gravity shift caused by

the weight of the powertrain. All other vehicle characteristics, such as weight of the chassis, wheel base, center of gravity, aerodynamic coefficients, etc., are considered parameters as they are based on the chassis of a Formula 3 race car. Despite the narrow focus of the case study, the work presented in [12] remarkably considers the optimal control problem within the design optimization. It does so by varying the steering angle, the braking torque applied on all four wheels and the driving torques applied on both rear wheels to find the optimal trajectory of the car around the track. The vehicle is model via a 7-degree of freedom (DOF) and the track is a planar version of the Nurburgring. The objective is to minimize the lap time of the vehicle. Like many of the works listed in the previous section, [12] seems to utilize a commercial monolithic approach. It also only considers the optimization of this race car's powertrain around a single track, resulting in the design's dependence on the track layout to not be studied.

Yu et al. build on the work they reported in [12] and extend it to a 4-IWD EV modelled via a 14-DOF vehicle model in [13]. The reasons for this extension were to take into account the effects of the unsprung mass of the wheel assembly. To this point, the authors also developed a "time-efficient" suspension model to characterize the relationships between the wheel jounce, spring and dampening forces, toe angle, steering angle and camber angle. With this suspension model, [13] analyzes the lap-time sensitivity to the mounting of the propulsion system (in-wheel vs. on-board) to determine which is better. Having determined that 4 in-wheel motors can achieve better lap-times, Yu et al. proceeded to use this propulsion system setup for vehicle optimization. Overall, the optimization problem presented in [13] is much more thorough as it not only considers the powertrain optimization problem described in [12] but also the following design variables: center of mass location, different pairs of motors for the front and rear axles (doubling the problem of [12]), both front and rear anti-roll bar coefficients, and the stiffness and dampening coefficients for the front and rear suspensions. Interestingly enough, [13] no longer considers the brake bias as a design variable and instead assumes that each wheel can achieve their independent optimal braking

force. That being said, like its predeceasing work, [13] seems to utilize the same commercial monolithic approach, only considers the optimization of the aforementioned variables around a single track and not consider any other discipline beyond the suspension.

To summarize, a gap exists in the literature on the optimization of EVs. First and foremost, there is no work that considers the design of the battery pack within an EV optimization problem. Secondly, the energy management topic is not examined. Thirdly, the existing literature does not seem to consider the relationship between the components of an electric powertrain (e.g., motors and battery) and the other disciplines present in a vehicle. Lastly, the EV optimization case studies seem to only use monolithic methods to solve the problem which would prevent the individual departments of MFE from owning their own design methods and working concurrently.

Chapter 3

Modeling

In this chapter, models used in the development of the MDO framework are described. More specifically, the models used to describe the competition, the lap simulation methodology, the subsystem models and other vehicle models needed to improve the accuracy of the lap simulations.

3.1 Competition model

In a typical FSAE competition, points are given to teams for their performance in static and dynamic events. The former evaluates the teams' soft-skills while the latter the performance capability of the developed vehicle. Only the dynamic events can be modelled and thus considered in the context of this optimization exercise. In total, there are 675 points given for dynamic events:

1. Acceleration
2. Skidpad
3. Autocross
4. Endurance

5. Efficiency

Each of these events aim to evaluate a different aspect of a vehicle's performance capabilities. The points awarded are based on the relative performance of the vehicle with respect to the other competing race cars. Unlike other motorsport competitions, different amount of points are awarded for each events. This is visually represented in Figures 3.1 and 3.5.

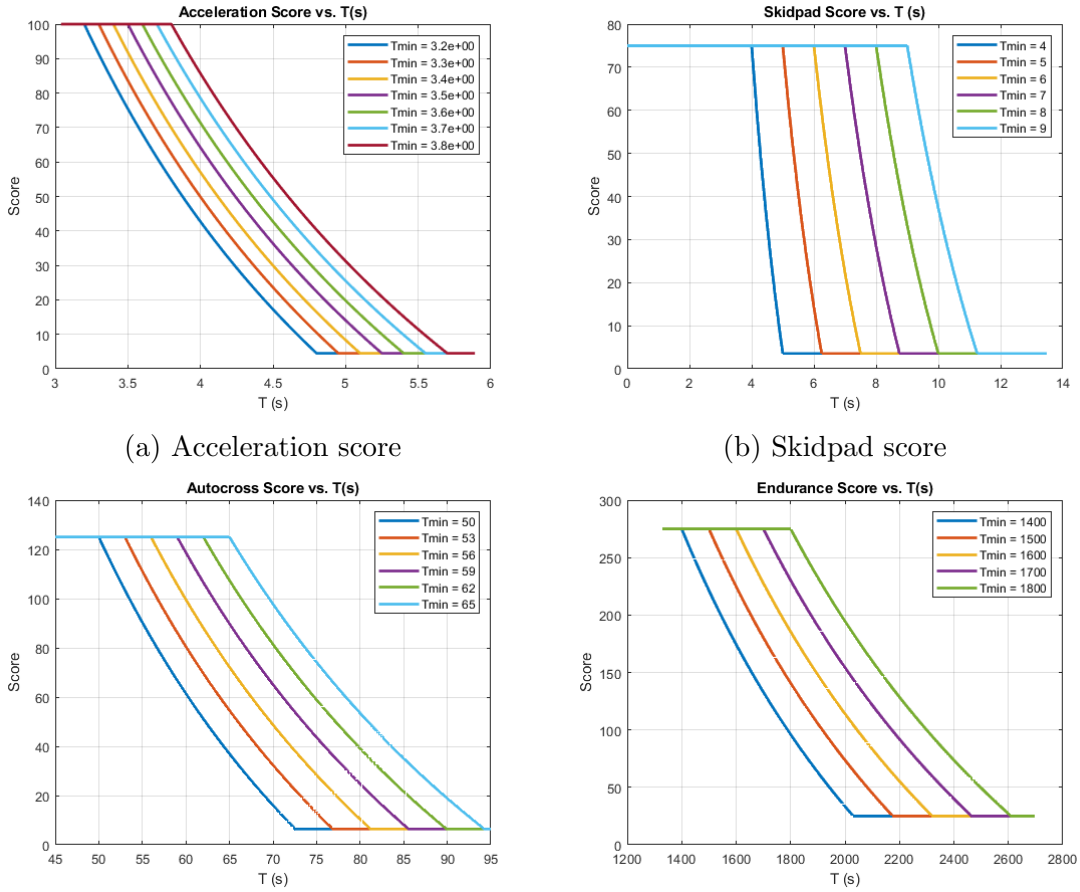

(a) Acceleration score

(b) Skidpad score

(c) Autocross score

(d) Endurance score

Figure 3.1: Scoring relative to t_{min}.

As these figures illustrate, the reference metric used for scoring can affect how points are awarded. For this reason, careful consideration was given in choosing these baseline values in order to avoid saturating the evaluation functions during the optimization process. If the functions were to saturate, distinguishing between designs would be impossible. With that said, the following subsections will describe each event, show how the points awarded are

calculated and provide the reference metric used.

3.1.1 Acceleration scoring

The acceleration event aims to evaluate a vehicle's ability to accelerate in a straight line on flat pavement. The length of the course is 75 meters. The scoring for this event is determined by

$$\text{Acceleration Score} = 95.5 * \frac{\frac{t_{max}}{t_{your}} - 1}{\frac{t_{max}}{t_{min}} - 1} + 4.5, \tag{3.1}$$

where t_{your} is the time for the team's vehicle to run the course, t_{min} the lowest time recorded across all participants and t_{max} is 150% of t_{min}.

From Equation (3.1), the maximum amount of points that a team can earn in this event is 100 points while the minimum is 4.5 points [1]. Figure 3.1a illustrates how the the value of t_{min} affects the scoring.

To choose an appropriate t_{min}, historical data from the Formula FSAE Lincoln competitions was analyzed. It was found that the lowest time for this event, of 3.687 seconds, was recorded during the 2019 competition [14]. Although this value can be used directly as the baseline value, it may not be representative as the rules guiding the vehicle design change year to year. Further, the lap simulations assume ideal conditions which tend to produce optimistic results. Simply using this value as the reference t_{min} would run the risk of saturating the function. For this reason, this best time was reduced by 10% to 3.318 seconds before being utilized as the value for t_{min} in the scoring of the acceleration event in this optimization study. The calculated score will be underestimated, but this is not important for the purpose of the optimization study so long as the designs can be distinguished. Using this value for t_{min} gives a value for t_{max} of 4.977 seconds.

3.1.2 Skid-pad scoring

The skid-pad event evaluates a vehicle's cornering ability during a constant radius turn. This is done by having the vehicle attempt to go around a circular track, whose middle diameter is 18.25 meters, clockwise and counter-clockwise as shown in Figure 3.2. The average time between the two is then used for scoring via the following equation

$$\text{Skidpad Score} = 71.5 * \frac{(\frac{t_{max}}{t_{your}})^2 - 1}{(\frac{t_{max}}{t_{min}})^2 - 1} + 3.5, \tag{3.2}$$

where t_{max} is 125% of t_{min}.

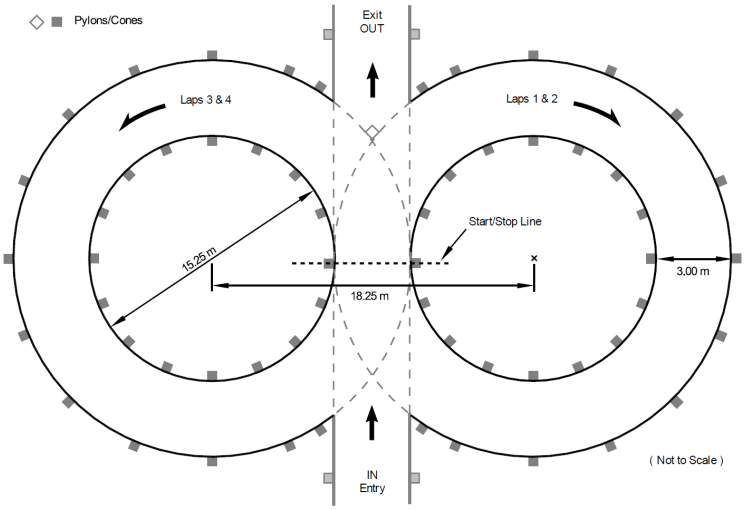

Figure 3.2: Skidpad track [1].

The maximum amount of points that a team can earn in this event is 75 points while the minimum is 3.5 points [1]. Figure 3.1b illustrates how the the value of t_{min} affects the scoring.

For similar reasons to the acceleration event, historical data from Formula FSAE Lincoln competitions was used to find an appropriate value for t_{min}. The best time found was 5.274 seconds which was recorded in 2018. This value was scaled down by 10% to 4.747 seconds to avoid any risk of saturating the scoring function and the resultant t_{max} value was 5.934 seconds.

3.1.3 Autocross scoring

The autocross event is used to assess a vehicle's maneuverability and handling over a single lap of a short tight course. Although the are many rules dictating the specifications of autocross courses, there is no fixed layout [1]. The track can change from year to year. The autocross track layout used in this work, shown in Figure 3.3, is the one from the 2018 Formula SAE Lincoln competition.

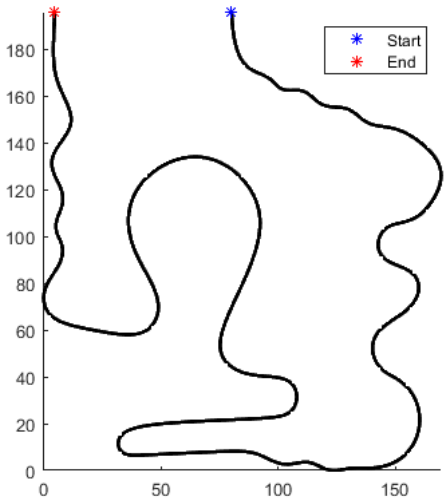

Figure 3.3: Autocross track layout.

This track was chosen simply because it is the only one accurately mapped by the university's FSAE team. The equation used to calculate the score for this event is

$$\text{Autocross Score} = 118.5 * \frac{\frac{t_{max}}{t_{your}} - 1}{\frac{t_{max}}{t_{min}} - 1} + 6.5, \tag{3.3}$$

where t_{max} is 145% of t_{min}.

The maximum amount of points that a team can earn in this event is 125 points while the minimum is 6.5 points [1]. The effects of t_{min} on the score is shown in Figure 3.1c.

Since the track is from the 2018 competition, only historical data from that year can be used. The best time, out of all 7 competitors that participated in the autocross event that

year, was 59.813 seconds. The small sample size of results further adds to the need to scale the historical value as the best result may not be representative of that of a competitive vehicle. Like the other events, simply doing a 10% scaling and using a t_{min} value of 53.832 seconds was sufficient to assure the function does not saturate. The resultant t_{max} was 78.056 seconds.

3.1.4 Endurance scoring

The endurance race is the event that most resembles a more "traditional" motorsports race. Cars do multiple laps around a given closed course to cover an approximate total distance of 22 km [1]. The goal of this event is to evaluate not only the performance of the vehicle but also test the durability and reliability. Like the autocross event, the endurance track can also change from year to year. The track that was used in this work, shown in Figure 3.4, is the one from the 2016 and 2017 Formula SAE Lincoln competitions. Vehicles have to complete 16 laps of this course to finish the event.

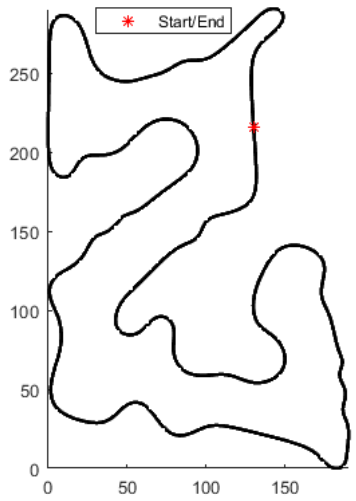

Figure 3.4: Endurance track layout.

Like the autocross track, this track was chosen simply because it is the only one for which the university's FSAE team had accurately mapped. The equation used to calculate

the score for this event is

$$\text{Endurance Score} = \begin{cases} 250 * \frac{\frac{t_{max}}{t_{your}} - 1}{\frac{t_{max}}{t_{min}} - 1} + 25, & \text{if event completed} \\ \text{Number of laps completed}, & \text{otherwise} \end{cases}, \tag{3.4}$$

where t_{max} is 145% of t_{min}.

The maximum amount of points that a team can earn in this event is 275 points while the minimum is 25 points[1] if the vehicle completes the event. The dependency of the score on the value of t_{min} is illustrated in Figure 3.1d. However, unlike the other events, if a team's vehicle begins the endurance round but is unable to complete the necessary required number of laps, a single point is awarded per lap completed.

Similar to the other events, a scaling of 15% was applied on the best historical time of 1490.355 seconds, recorded in 2017, to avoid saturating the scoring function. The baseline, t_{min}, that was used 1266.80 seconds and the resultant t_{max} was 1836.86.

3.1.5 Efficiency scoring

The efficiency event differs greatly from the others. It is based on both the average lap-time and average equivalent kg of CO_2 used per lap during the endurance event. These average values are used to determine the efficiency factor η of the vehicle which is then used to calculate the efficiency score. The energy used by the vehicle is converted to kg of CO_2 using the factor 0.65 kg of CO_2 per kWh [1]. The equation for the efficiency factor is given by

$$\eta = \underbrace{\frac{t_{avg_{min}}}{t_{avg_{your}}}}_{\text{Average Lap Time Factor}} * \underbrace{\frac{CO_{2_{avg_{min}}}}{CO_{2_{avg_{your}}}}}_{\text{Average Energy Factor}}, \tag{3.5}$$

where $t_{avg_{min}}$ is the minimum average endurance lap-time, $t_{avg_{your}}$ is the team's vehicle average endurance lap-time, $CO_{2_{avg_{min}}}$ is the minimum average kg of CO_2 used per endurance lap and $CO_{2_{avg_{your}}}$ is the team's vehicle average kg of CO_2 used per endurance lap. The equation

for the efficiency score is given by

$$\text{Efficiency Score} = \begin{cases} 0, & \text{if } t_{avg_{your}} > 1.45 t_{avg_{min}} \\ 0, & \text{if } CO_{2_{avg_{your}}} > 0.8259\text{kg per lap} \cdot \\ 100 * \frac{\eta_{min}/\eta_{your}-1}{\eta_{min}/\eta_{max}-1}, & \text{otherwise} \end{cases} \tag{3.6}$$

As Figure 3.5 illustrates, although the endurance score depends on both the average lap-time and energy usage, it is far less sensitive to lap times.

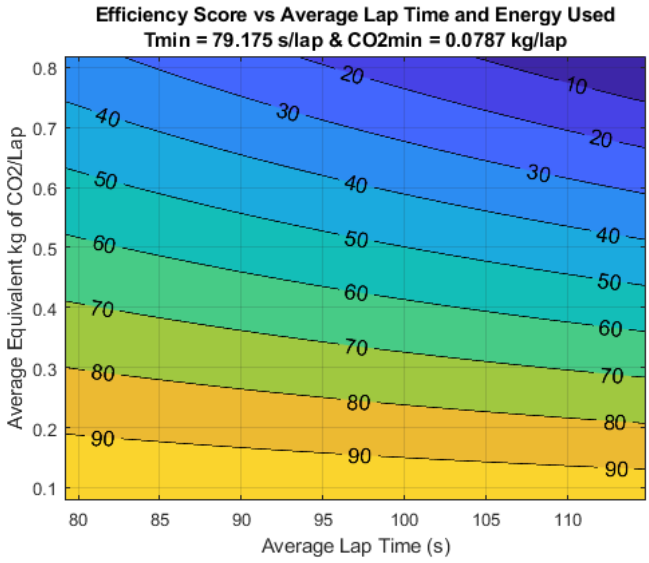

Figure 3.5: Efficiency points vs average CO_2 and lap time.

Since the efficiency score is based on the endurance event, the 2017 Formula FSAE Lincoln results were also used as reference. Using the adjusted baseline time of 1266.80 seconds for the endurance event, the minimum average endurance lap-time, $t_{avg_{min}}$, was 79.175 seconds. The $CO_{2_{avg_{min}}}$ recorded in 2017 was 0.1109 kg of CO_2 per lap. Keeping the same use of a 15% adjustment as the endurance event, this gave an adjusted value of 0.0943 kg of CO_2 per lap.

As per the rules, the minimum efficiency factor was calculated with a $t_{avg_{your}}$ value of 1.45 times $t_{avg_{min}}$, in this case 114.804 seconds, and a $CO_{2_{avg_{your}}}$ value of 0.8259 kg of CO_2 per lap [1]. Using these values yielded a minimum efficiency factor of 0.0787.

The maximum efficiency factor can be anything between the minimum value and 1. For the maximum efficiency factor to be equal to 1, a team must have both the minimum average endurance lap-time and the minimum average equivalent kg of CO_2 used per lap. For simplicity, in this work, it was assumed that the maximum efficiency factor is 1.

From Equation (3.6), the maximum amount of points that a team can earn for their efficiency during the endurance event is 100 points while the minimum is 0. Unlike the evaluation methods of the other events, if the vehicle's average endurance lap-time exceeds 1.45 times the minimum average time, the team receives zero points. Similarly, if a team's vehicle consumes more than 0.825 kg of CO_2 per lap, the team scores zero points in the event.

3.2 Vehicle models

In order to evaluate the designs, lap simulations are used. To develop these simulations with the desired fidelity, models are required to characterize the vehicle.

Above all, a method for determining the loads at the contact patches, the portion of the tire that is in contact with the road surface, is necessary. Fortunately, MFE had previously developed a tire model based on the Magic Formula presented in [15] and fitted with test data from the Tire Test Consortium [16] for the "Hoosier 18.0x6.0 LCO 7in" tire. This tire model is represented graphically in Figure 3.6.

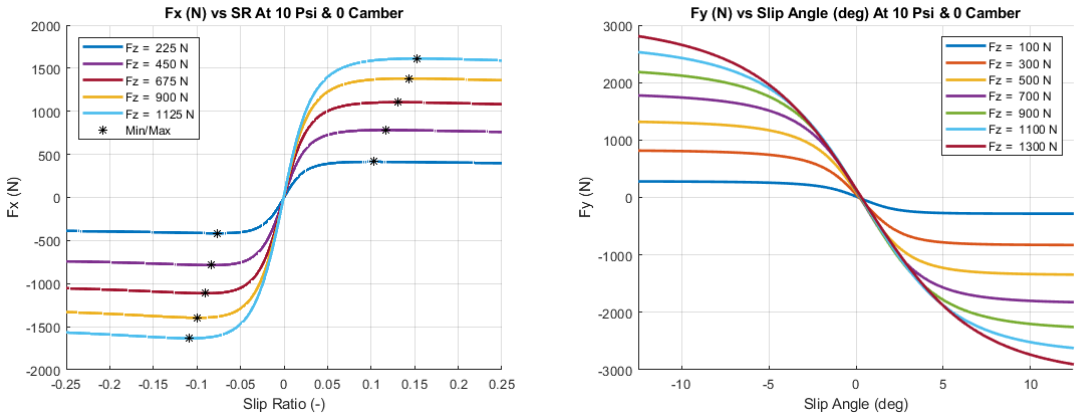

(a) Longitudinal pure slip model. (b) Lateral pure slip model.

Figure 3.6: Hoosier 18.0x6.0 LCO 7in tire model.

Assuming that the control systems and driver would be able to consistently keep the tires in their optimal operating range, the tire model was simplified by removing the the slip ratio and slip angles dimensions. The maximum loads that the tire can produce was made a function of the vertical load on the tire as shown in Figure 3.7. This simplified tire model is used in the lap simulations.

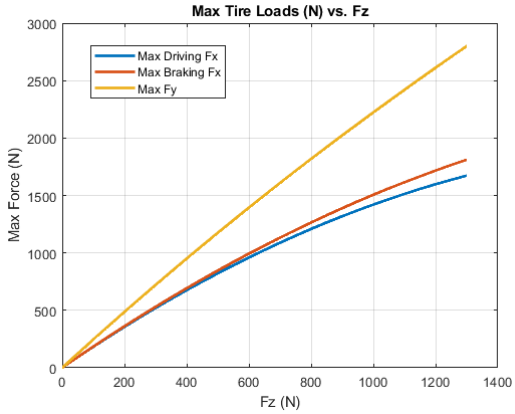

Figure 3.7: Simplified tire model.

Moreover, a model is needed to describe the characteristics of the AMK motors used. Using manufacturer data, the university's FSAE team developed motor torque and efficiency curves with an inverter input of 600VDC. These are shown in Figure 3.8.

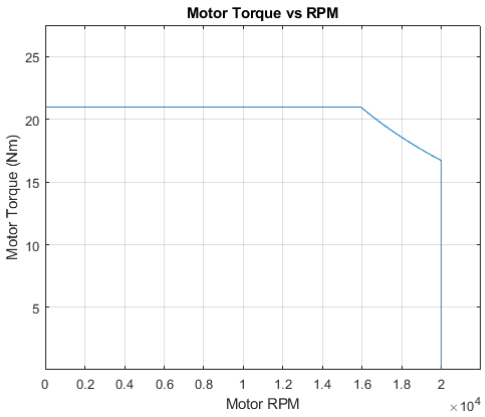

(a) AMK motor torque curve.

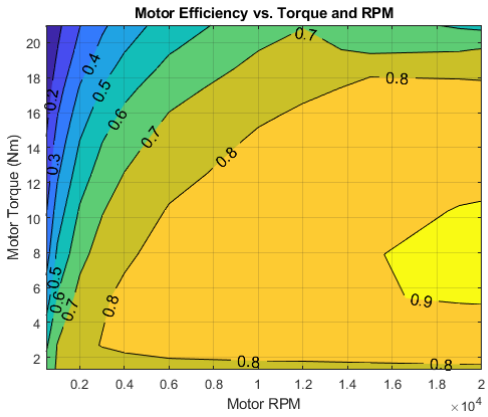

(b) Contour plot of AMK motor efficiency.

Figure 3.8: AMK motor characteristics at 600V.

With regards to the vehicle suspension, the difference between the static ride heights and ride heights under race loads needs to be estimated. This is important to get a better estimate of the aerodynamic loads around the track. Using the provided values for the front and rear spring stiffness and motion ratios, the developed ride height model uses Hooke's law. This simple method is chosen as the lap simulation method developed for this framework does not consider transient information. Therefore, the effects of dampening are neglected.

The other vehicle characteristics are represented via the properties given in Table 3.1 below. It is important to note that the optimization process will affect the total unsprung and sprung mass, which will in turn affect the center of gravity of the vehicle. Given this, the values for the mass related properties given below are only valid with the initial state of the subsystems being optimized.

Table 3.1: Summary of vehicle parameters.

Parameters	**Values**
Wheel Base [m]	1.5250
Track Width [m]	1.1176
Lateral Load Transfer Distribution	0.4258
Heave Motion Ratio Front	1.2500
Heave Motion Ratio Rear	1.2823
Heave Spring Stiffness Front [N/m]	52538.0505
Heave Spring Stiffness Rear [N/m]	61294.3923
Inverter Efficiency	0.9800
Baseline Total Unsprung Mass [kg]	60.6900
Baseline Total Sprung Mass [kg]	130.4000
Driver Mass [kg]	70.0000
Baseline Center of Gravity (Unsprung) [m, m, m]	[0.7625, 0.5588, 0.2032]
Baseline Center of Gravity (Sprung) [m, m, m]	[0.7015, 0.5588, 0.3000]
Baseline Center of Gravity (Total) [m, m, m]	[0.7157, 0.5588, 0.2775]

3.3 Subsystem models

In this work, the subsystems that were included into the MDO framework are the external aerodynamics, accumulator and geartrain. In this section, the modeling approach for the subsystems will be described. The external aerodynamics and accumulator models were developed specifically for this optimization study, while the gear train model was provided by the university's FSAE team.

3.3.1 External aerodynamics

The external aerodynamics is an interesting subsystem to optimize as it affects various performance characteristics of the vehicle. Mostly importantly, the downforce produced by the aerodynamic package increases the observed weight on the tires. This has the effect of increasing the maximum loads that the tires can produce, as is shown in Figures 3.6 and 3.7, without increasing the mass of the vehicle. However, this does not come freely. Drag is a major source of energetic loss and reduces the range, and thus efficiency, of the vehicle. Moreover, FSAE race cars can be sensitive to ground effects meaning vehicle attitude is also important in the estimation of aerodynamic loads.

That being said, to optimize the aerodynamic system, the model for this subsystem considers the possible design configurations and the various potential states of the vehicle. For this work, the design variables chosen are the angle of attack (AoA) of the third front element (α_{F3}), second rear element (α_{R2}) and third rear element (α_{R3}) as shown in Figure 3.9. The state variables are the speed of the car and the front and rear ride height. The desired outputs to properly characterize the effects of these variables on the performance of the vehicle are the coefficient of lift, the coefficient of drag and the longitudinal aerodynamic force distribution.

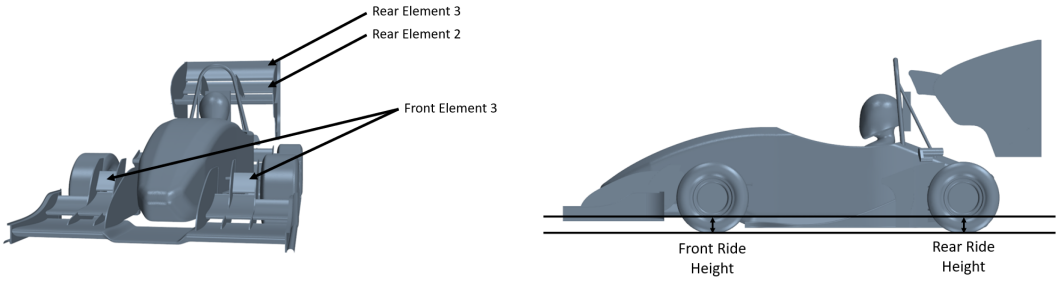

Figure 3.9: Simplified vehicle CAD model.

To build such a model, an understanding of the relationship between the design and state variables and output is needed. This was achieved by conducting a design of experiment.

More specifically, 600 samples from the design space were randomly picked via a Latin hypercube sampling process. A half vehicle, with symmetry, steady-state computational fluid dynamics (CFD) simulation.

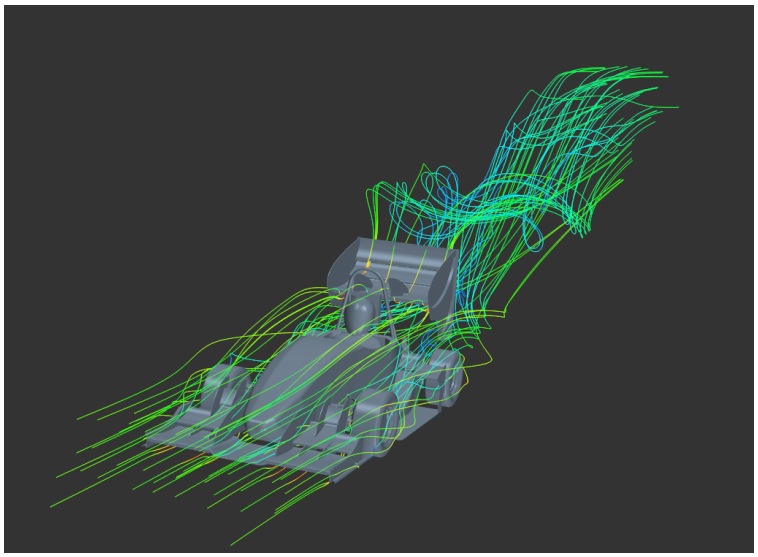

Figure 3.10: External aerodynamics velocity streamlines.

The data obtained by the CFD simulations was then used to build a Kriging meta-model. This was done to construct a sufficiently accurate representation of the entire design space without needing to run additional computationally expensive CFD simulations. This was particularly important as this subsystem model was constantly queried during the lap simulations.

3.3.2 Accumulator

The accumulator or battery pack, is the primary power source of electric vehicles. These battery packs are composed of individual battery cells interconnected both in parallel and in series to achieve the high energy capacity, voltage and power required in EV applications. The connected cells form a module which in turn are connected together to make the battery pack [17]. An example of a module and battery pack container arrangement considered by MFE is illustrated in Figure 3.11.

The design of the battery pack depends on the cell type used (T_C), the number of cells connected in parallel (n_{C_P}), the number of these parallel bundles in a module widthwise ($n_{C_{MW}}$) and lengthwise ($n_{C_{ML}}$), and the number of modules in the battery pack widthwise (n_{MW}) and lengthwise (n_{ML}). Each possible cell type have their own voltage (V_{cell}), dimensions, peak discharge ($I_{discharge_{cell}}$) and charge ($I_{charge_{cell}}$) currents and capacity (C_{cell}). Six different pouch cells are considered from the manufacturers *Thunder Power RC* and *Shenzhen Malesta Battery Co.* These design variables affect the accumulator's dimensions, available energy, discharge power, charge power and mass. As a result, this subsystem directly dictates the vehicle's power and energy recovery capabilities, has consequences on the range and also impacts the dynamics of the vehicle through its effects on the center of gravity.

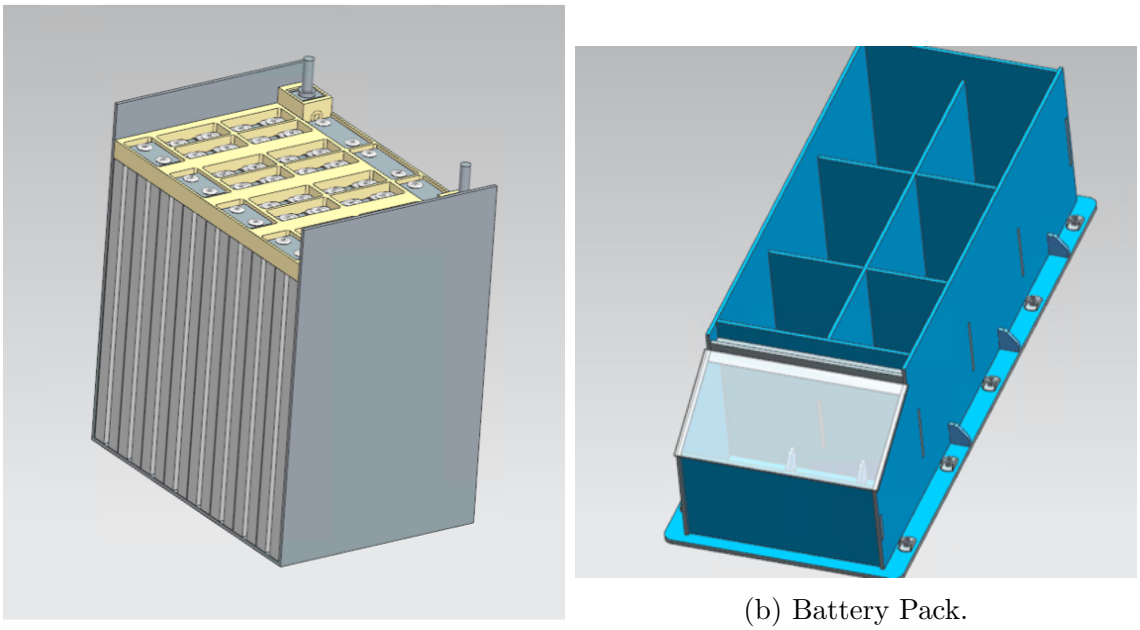

(a) Module.

(b) Battery Pack.

Figure 3.11: Example CAD model of module and battery pack.

For this reason, the accumulator model takes as input the six design variables described above and outputs the battery's pack voltage (V_A), energy (E_A), maximum discharge ($P_{discharge}$) and charge (P_{charge}) powers, length (L_A), width (W_A), height (H_A), mass (m_A) and finally, volumetric energy density (E_d). This last output is used as the optimization

objective described in Subsection 4.2.1. Ohm's and Joule's laws are used to calculate the electrical properties of the battery pack depending on the chosen cell as shown by the following equations

$$n_{C_S} = n_{C_{MW}} * n_{C_{ML}} * n_{ML} * n_{MW}, \tag{3.7}$$

$$P_{discharge} = I_{discharge_{Cell}} * n_{C_P} * V_{cell} * n_{C_S}, \tag{3.8}$$

$$P_{charge} = I_{charge_{Cell}} * n_{C_P} * V_{cell} * n_{C_S}, \tag{3.9}$$

$$V_A = V_{cell} * n_{C_S}, \tag{3.10}$$

$$E_A = C_{cell} * n_{C_P} * V_A, \tag{3.11}$$

$$E_d = \frac{E_A}{L_A * W_A * H_A}, \tag{3.12}$$

where n_{C_S} is the number of cells in series.

The physical properties of the accumulators are obtained by simply multiplying a given physical dimension or mass of the chosen cell by the number of cells.

3.3.3 Gear train

The gear train used in MFE's electric race car is a two-stage planetary gear train for which an example is shown in Figure 3.12. Each of the four in-wheel motors has their own gear train. The input of the gear train is the sun gear while the output can be either the ring gear or second stage planet carrier.

This subsystem is important for multiple reasons but primarily because the final gear ratio impacts the tractive and regenerative torques and can limit the speed of the vehicle. In addition, the gear train's mass affects the unsprung mass of each corner, and in consequence, the overall center of gravity. Finally, considering that the race vehicle being optimized has each wheel independently driven, the flexibility of having different pairs of gear trains for the front and rear motors was also of interest.

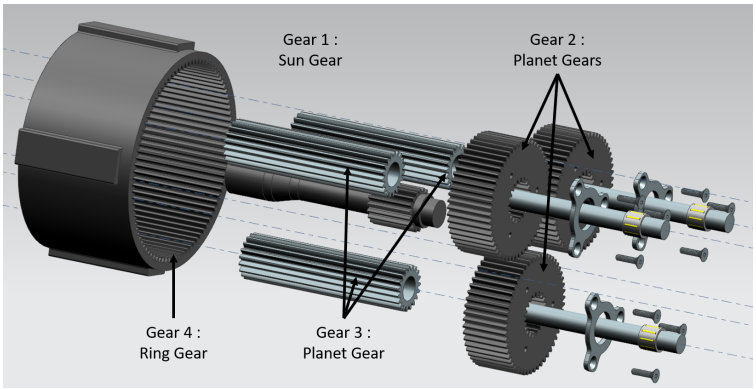

Figure 3.12: Annotated gear train with ring gear as output.

To understand the impacts of the design of the gear train on the vehicle, the model for this subsystem outputs the mass, gear ratio and outer diameter for a given design. Moreover, it also considers the durability of each of the gears in the gear train to determine if the design is suitable for the loads they will sustain.

To characterize the gear stresses, MFE used the AGMA stress and fatigue strength equations to calculate the bending and surface stresses [18]. Utilizing the autocross track described in Subsection 3.1.3, a load case was developed from a baseline lap simulation. The lap simulation used to get this baseline load case was different and less detailed than the one described in Section 3.4 which was developed for this work. The autocross track was chosen by MFE as it was found it was the most demanding course on the gears. From this baseline lap simulation, a heat-map of the frequencies of the torques applied by the motor at a given RPM shown was produced. Evidently, being able to complete a single autocross event would not be sufficient. Therefore, the load case was extended to cover about 440 autocross events, greatly overestimating the use the gears will be subjected to during an entire race season. MFE then made use of the Palmgren-Miner rule to evaluate the fatigue cumulative damage on the gears.

That being said, the developed model takes as input the diametral pitch (DP_1, DP_2), the number of teeth (n_{T_1}, n_{T_2}, n_{T_3}, n_{T_4}) and the face width (F_{W_1}, F_{W_2}) for each of the four gears shown in Figure 3.12. In addition, it also takes as input a Boolean flag to chose the

output gear (O_{RG}). As alluded to previously, the outputs are the gear ratio (GR), mass (m_{gear}), outer diameter (d_o) and the bending and surface cumulative damage (D_{CB_1}, D_{CB_2}, D_{CB_3}, D_{CB_4}, D_{CS_1}, D_{CS_2}).

3.4 Lap simulation

To evaluate the performance of vehicles, and therefore be able to compare the designs generated by the optimization process, a lap simulation methodology was developed specifically for this work. The output of the lap simulations is used, in conjunction with the event models described in Section 3.1, to determine the points scored. A high-level overview of how the lap simulations fit within the MDO framework is shown in Figure 3.13 with further details given in Chapter 4. At every iteration i of the MDO process, a fixed design of the system and subsystems $\widetilde{\mathbf{x}}_{veh}$ is used by the lap simulations to determine the event scores. These scores are then used by the optimizer to produce a new design iterate. The process is repeated until a termination criteria is met.

Figure 3.13: Interrelationship between the MDO and lap simulation processes.

The chosen simulation methods are based on a quasi-steady-state approach that determines the velocity, and longitudinal and lateral accelerations around a circuit by subdividing it into small sections [19]. In the developed simulation algorithms, each track section is a

characterized by a curvature and length. At each of these segments, the vehicle's velocity and accelerations are calculated via a two-track vehicle model at equilibrium. These track sections are then stitched together to determine the time to complete the circuit.

Although the developed method provides a way of determining which design is better, it does have a couple of limitations. The first being that transient behaviour of the vehicle is ignored. The second is that the effects of design changes on the optimal trajectory are not considered. In consequence, any potential performance differences resulting from a vehicle being able to take a better trajectory cannot be computed.

To implement the quasi-steady-state method found in this work, two auxiliary optimization problems were formulated and are solved at every track segment s. The first problem finds $v^s_{x_{Max}}$, the steady-state maximum speed the vehicle can travel on a given segment with a certain radius r and fixed vehicle and subsystem design $\widetilde{\mathbf{x}}_{veh}$. This is achieved by treating the maximum speed as an independent variable. The constraints are that no motor can exceed it's RPM limit, no motor can exceed it's torque limit at the given RPM, no tire can exceed it's traction capability and finally, the vehicle power usage cannot exceed the imposed limit or battery limit and finally. One of these nonlinear inequality constraints is known to be active but identifying which ahead of time, and at what value of $v^s_{x_{Max}}$, is not possible without solving this problem. The problem formulation, with the radius at a given segment and vehicle design being parameters is

$$\begin{aligned}
\min_{v^s_{x_{Max}}} \quad & -v^s_{x_{Max}} \\
\text{s.t.} \quad & \frac{F_{x_{Tire}}(v^s_{x_{Max}};\widetilde{\mathbf{x}}_{veh},r(s))^2}{F_{x_{Tire_{Max}}}(v^s_{x_{Max}};\widetilde{\mathbf{x}}_{veh},r(s))^2}+\frac{F_{y_{Tire}}(v^s_{x_{Max}};\widetilde{\mathbf{x}}_{veh},r(s))^2}{F_{y_{Tire_{Max}}}(v^s_{x_{Max}};\widetilde{\mathbf{x}}_{veh},r(s))^2}-1\leq 0 \\
& \tau_{Motor}(v^s_{x_{Max}};\widetilde{\mathbf{x}}_{veh},r(s))-\tau_{Motor_{Max}}(v^s_{x_{Max}};\widetilde{\mathbf{x}}_{veh},r(s))\leq 0 \\
& \dot{\theta}_{Motor}(v^s_{x_{Max}};\widetilde{\mathbf{x}}_{veh},r(s))\leq \dot{\theta}_{Motor_{Max}} \\
& P(v^s_{x_{Max}};\widetilde{\mathbf{x}}_{veh},r(s))-P_{Max}\leq 0
\end{aligned} \quad , \tag{3.13}$$

where $\dot{\theta}_{Motor}$ is the angular velocity of each motor, $\dot{\theta}_{Motor}$ is the tractive or regenerative

torque for each motor, P is the total power drawn or regenerated by the motors, $F_{x_{Tire}}$ is the longitudinal force applied at the contact patch of each tire and $F_{y_{Tire}}$ is the lateral force applied at the contact patch of each tire.

The second optimization problem maximizes the traction or braking motor torques, across all four tires, in order to either maximize acceleration or regenerative braking of the vehicle on a track segment. These torques are then used to find the speed that the vehicle will have at the next track segment $v_x^{(s+1)}$. To do this, the maximum speed at segment $s+1$, which can be determined using the problem shown in Equation (3.13), is used as an acceleration or braking target. Using previous variable definitions, the problem formulation is

$$\begin{aligned}
\min_{\boldsymbol{\tau}} \quad & -(\tau_{FL} + \tau_{FR} + \tau_{RL} + \tau_{RR}) \\
\text{s.t.} \quad & v_x^{(s+1)} - v_{x_{Max}}^{(s+1)} \leq 0 \\
& \frac{F_{x_{Tire}}(\boldsymbol{\tau}; \widetilde{\mathbf{x}}_{veh}, r(s), v_x^s)^2}{F_{x_{Tire_{Max}}}(\boldsymbol{\tau}; \widetilde{\mathbf{x}}_{veh}, r(s), v_x^s)^2} + \frac{F_{y_{Tire}}(\boldsymbol{\tau}; \widetilde{\mathbf{x}}_{veh}, r(s), v_x^s)^2}{F_{y_{Tire_{Max}}}(\boldsymbol{\tau}; \widetilde{\mathbf{x}}_{veh}, r(s), v_x^s)^2} - 1 \leq 0 \\
& \tau_{Motor}(\boldsymbol{\tau}; \widetilde{\mathbf{x}}_{veh}, r(s), v_x^s) - \tau_{Motor_{Max}} \leq 0 \\
& P(\boldsymbol{\tau}; \widetilde{\mathbf{x}}_{veh}, r(s), v_x^s) - P_{Max} \leq 0 \\
& \dot{\theta}_{Motor}(\boldsymbol{\tau}; \widetilde{\mathbf{x}}_{veh}, r(s), v_x^s) \leq \dot{\theta}_{Motor_{Max}}
\end{aligned}, \tag{3.14}$$

with

$$\boldsymbol{\tau} = [\tau_{FL}, \tau_{FR}, \tau_{RL}, \tau_{RR}] \tag{3.15}$$

where τ_{FL} is the tractive or regenerative torque for front left motor, τ_{FR} is the tractive or regenerative torque for front right motor, τ_{RL} is the tractive or regenerative torque for rear left motor, τ_{RR} is the tractive or regenerative torque for rear right motor and v_x^s is the actual vehicle speed at location s.

3.4.1 Acceleration

Simulating the acceleration event is straightforward. The straight track is divided into segments on which the vehicle accelerated from a standing start. The division of the track is done in three parts to improve the accuracy of the results. The first meter is divided into segments of 0.005 m. The next 5 meters has sections of 0.01 m and the rest of the track is cut up in 0.1 m parts. By doing this, the behaviour of the vehicle, initially traction limited at the start of the event, is captured.

The simulation utilizes the function which solves the problem given by Equation (3.14) to find the acceleration and speed at every section. The total time is then determined by stitching together the speeds and track segment lengths.

3.4.2 Skid-pad

From the description in Subsection 3.1.2, the skid-pad event can be represented as a circle with a radius of 9.125 m. The maximum speed around this constant radius turn is obtained by using the radius as a parameter in the problem detailed in Equation (3.13). It is assumed that the vehicle would be able to get to this speed as it begins its circular trajectory. Using the calculated maximum constant speed and knowing the circumference of the track, the estimated time to complete the event is calculated.

3.4.3 Autocross & endurance

The lap simulations methodology for the autocross and endurance events are mostly the same. The process is split into three steps. Using the autocross event as an example, Figure 3.14 shows the flowchart of the lap simulation procedure.

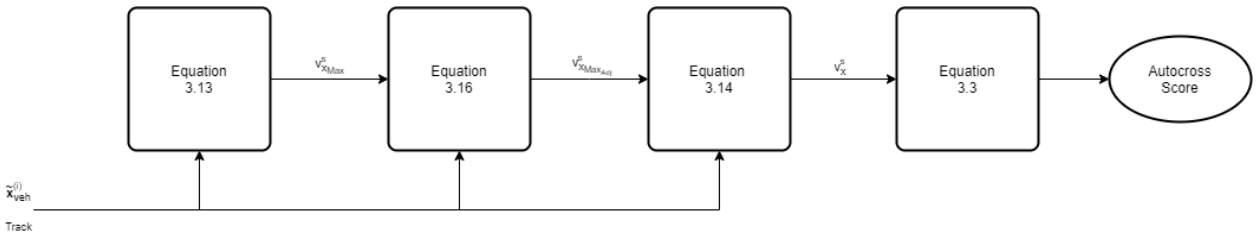

Figure 3.14: Autocross lap simulation flowchart.

The first step is to find the steady-state maximum speeds at every point on a given track. This step solves the problem given by Equation (3.13) at each point by providing the vehicle design and the track radius at the given location. An example of the results at the end of this stage is shown in Figure 3.15a. As this figure illustrates, there are harsh transitions from high to low speeds which are not physically possible.

These maximum speeds need to be adjusted to account for the braking capability of the vehicle. Assuming that the brakes alone could provide the necessary braking torques required to saturate the tire capabilities, the adjusted maximum speeds, $v^s_{x_{Max_{Adj}}}$, are found by solving the problem

$$\begin{aligned}
\min_{v^s_{x_{Max_{Adj}}}} \quad & -v^s_{x_{Max_{Adj}}} \\
\text{s.t.} \quad & \frac{(F_x(v^s_{x_{Max_{Adj}}}; \widetilde{\mathbf{x}}_{veh}, r(s), v^{(s+1)}_{x_{Max_{Adj}}}) - F_{Dr}(v^s_{x_{Max_{Adj}}}; \widetilde{\mathbf{x}}_{veh}, r(s)) - F_{Roll}(v^s_{x_{Max_{Adj}}}; \widetilde{\mathbf{x}}_{veh}, r(s)))^2}{F_{x_{Tire_{Max}}}(v^s_{x_{Max_{Adj}}}; \widetilde{\mathbf{x}}_{veh}, r(s), v^{(s-1)}_{x_{Max_{Adj}}})^2} + \\
& \frac{F_{y_{Tire}}(v^s_{x_{Max_{Adj}}}; \widetilde{\mathbf{x}}_{veh}, r(s))^2}{F_{y_{Tire_{Max}}}(v^s_{x_{Max_{Adj}}}; \widetilde{\mathbf{x}}_{veh}, r(s), v^{(s-1)}_{x_{Max_{Adj}}})^2} - 1 \leq 0 \\
& v^s_{x_{Max_{Adj}}} - v^s_{x_{Max}} \leq 0
\end{aligned} \tag{3.16}$$

where F_x is the required braking force and $v^s_{x_{Max}}$ is the steady-state maximum speed at s given by Equation (3.13).

Similar to problem (3.13), (3.16) treats $v^s_{x_{Max_{Adj}}}$ as an independent variable while also being the desired output. The segment radius and vehicle design are parameters.

This stage of the lap simulation process is completed in an iterative manner as the result depends on the vehicle state at three different track positions ($s-1$, s, $s+1$). Following the

same autocross example, the maximum speeds after this step are shown in Figure 3.15b.

Having the adjusted steady-state maximum speeds, simulating the vehicle around the track is now possible. The adjusted maximum speeds obtained with Equation (3.16) are passed onto the problem given by Equation (3.14) to determine the actual speeds that the vehicle achieves during the events. As such, the results of this step is what is used to determine the scores for the autocross and endurance events. An example of the resulting speed profile is shown in Figure 3.15c.

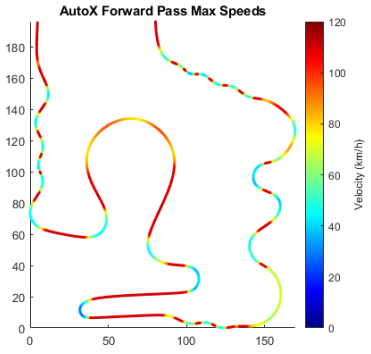

(a) Initial approximation of maximum speeds.

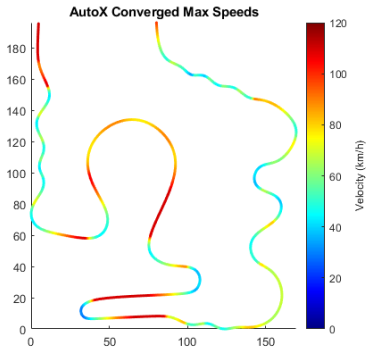

(b) Converged max speeds.

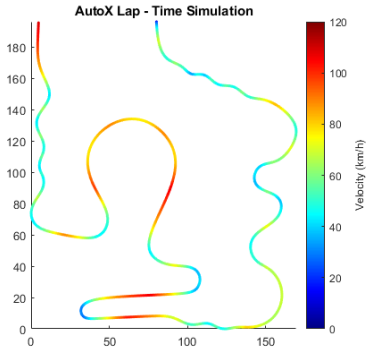

(c) Final speed profile.

Figure 3.15: Autocross speed profile at different lap simulation steps.

For the autocross event, the total time to complete the course is determined by utilizing the track segment length and speed at each point on the track. However for the endurance event, additional work is needed to account for the fact that the vehicle does multiple laps of the track. To do this, two lap simulations are done. The first from a standing start and the

second from a running start which utilized the final calculated speed of the standing start simulation. Considering that [1] dictates that a driver change is required half way through the endurance event and there are 16 laps to complete, the total time to complete the event is estimated by summing two standing lap times and 14 running lap times. Further, the energy utilized and regenerated at every step of the two endurance lap simulations is summed to estimate how many laps the vehicle was able to complete. The total time is then adjusted if the vehicle was unable to complete the event. Also, a different scoring method is used based on whether or not the vehicle was able to complete the 16 required laps as is explained in Subsection 3.1.4. With the standing and running lap times calculated and having estimated the number of laps the vehicle can complete, the average lap time and average energy used per lap is calculated in order to determine the efficiency score.

Chapter 4

Multidisciplinary Design Optimization Framework

The development of the optimization framework for MFE depends on the selected MDO architecture. Due to the different requirements set forth by the team regarding distribution of the optimization tasks and having the ability to add new subsystems to the framework, the analytical target cascading architecture was chosen. This particular architecture is capable of coordinating constraints between subsystems, distributing the different subsystem optimization tasks and can be adapted to consider a general objective function [3, 6]. Although many of the design coordination capabilities of ATC were not utilized in this work due to the lack of direct coupling between the three subsystems chosen, this architecture will be capable of accommodating any expansion of the developed framework by MFE. An added benefit of ATC is the fact that it is an individual discipline feasible (IDF) architecture [3]. As such, it can produce feasible subsystem designs even if the coupling constraints are not satisfied. This feature could allow McGill Formula Electric to potentially consider designs that are infeasible at the system level and attempt to make them feasible through slight redesigns.

The optimization algorithm chosen for the entire framework was the mesh adaptive direct

search (MADS) [20]. More precisely, the MATLAB version of the NOMAD software was utilized which implements the MADS algorithm. This algorithm was chosen for its capabilities with handling problems with no derivatives, for being able to work with all types of variables (continuous, discrete and categorical) and finally, for dealing with infeasible designs.

This chapter will describe in greater detail the MDO framework developed, shown in the extended design structure matrix (XDSM) in Figure 4.1 [21], by explaining the system and subsystem optimization problems.

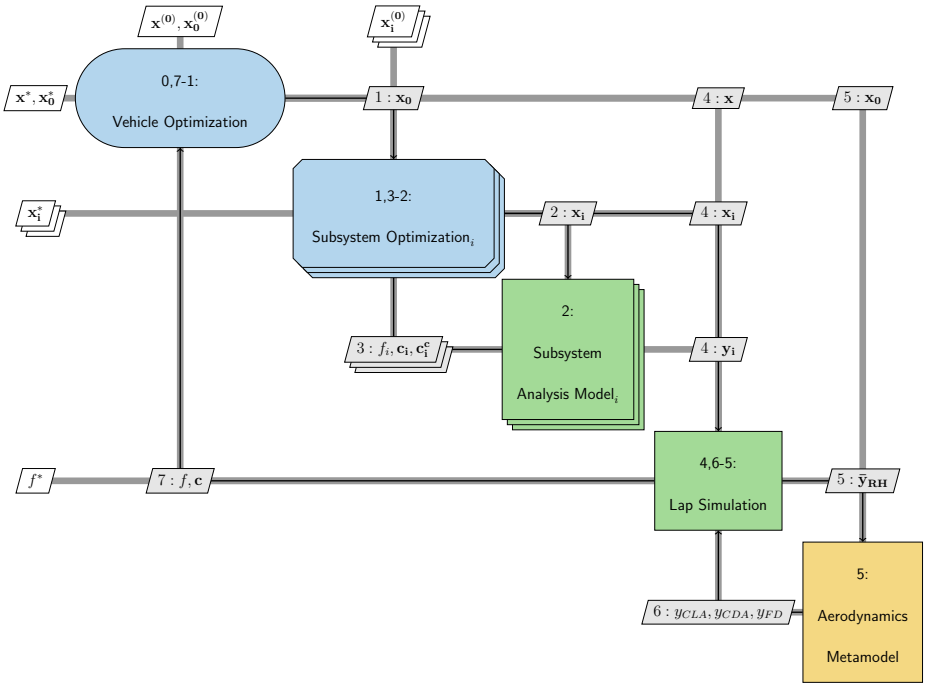

Figure 4.1: XDSM of optimization and analysis framework.

4.1 Vehicle-level optimization

The objective of vehicle level or system level optimization problem was to score the most amount of points as possible. This was achieved by coordinating the optimization of the external aerodynamics, accumulator and gear train subsystems while also optimizing certain system level variables.

In this work, the vehicle level optimizer provided targets to the subsystem level optimiza-

tion problems which were then used as constraints in the subsystem optimization problems. That is, instead of using consistency constraints at the system level, the consistency of the design was maintained by the subsystem. In particular, the vehicle optimization problem provided the gear train optimizer a gear ratio target for the front and rear gear trains (GR_{F_T}, GR_{R_T}) and the battery optimizer a minimum charge power ($P_{charge_{min}}$), energy target (E_T) and voltage target (V_T). Since the models for the motor torques and efficiencies were only valid for a 600 VDC input, the voltage target was a parameter of the vehicle optimization study. The energy targets and minimum charge power variables were needed to give flexibility to the optimizer and evaluate a potential trade-off between capacity and power regeneration capabilities.

Due to the current lack of direct coupling between subsystem, the only way of quantifying the effects of the aerodynamic variables was directly through the lap simulations. For this reason, the variables for this subsystem were brought up to the vehicle level and were controlled by the vehicle optimizer. Besides the above mentioned targets and aerodynamic subsystem variables, the system also had as a variable the power limit (P_{limit}) for the vehicle. Using prior knowledge of the problem, the problem was simplified by using the power limit as a variable for only the endurance simulations while the other three events simply used the maximum power allowed by the rules (80 kW) [1]. This was done because the energy consumption during the acceleration, skid-pad and autocross events is relatively insignificant to the energy available in the battery pack and there is no need to trade-off acceleration and speed for range.

Given the above, the vehicle level problem formulation is.

$$\begin{aligned} \min_{\mathbf{x}_{veh}} \quad & -score(\mathbf{x}_{veh}; V_T) \\ \text{s.t.} \quad & \mathbf{x}_{veh_{Min}} \leq \mathbf{x}_{veh} \leq \mathbf{x}_{veh_{Max}} \end{aligned} \tag{4.1}$$

with

$$\mathbf{x}_{veh} = [GR_{F_T}, GR_{R_T}, \alpha_{F3}, \alpha_{R2}, \alpha_{R3}, P_{charge_{min}}, E_T, P_{limit}] \tag{4.2}$$

$$\mathbf{x}_{veh_{Min}} = [5, 5, -4, -4, -4, 0, 3000, 10000] \tag{4.3}$$

$$\mathbf{x}_{veh_{Max}} = [20, 20, 4, 4, 4, 120000, 8000, 80000] \tag{4.4}$$

$$V_T = 600 \tag{4.5}$$

Due to the nature of the optimization problem at hand, the above process ran the risk of having its subsystem optimizers fail to find feasible subsystem designs which match the provided targets. The vehicle optimization process would then be unable to proceed unless the chosen system optimizer was robust to infeasible designs. As mentioned previously, one of the reason the MADS algorithm was chosen is because it negates this risk by being capable of handling infeasible designs.

4.2 Subsystem-level optimization

4.2.1 Accumulator

The optimization of the accumulator centers around finding the battery design which produces the highest volumetric energy density while fitting within the geometric constraints, meeting the voltage and energy targets, and respecting the minimum discharge and charge power capabilities. In more detail, the accumulator needed to fit in a prescribed volume within the chassis of the vehicle. These geometric constraints directly restricted the length, width and height of the battery pack and provide limits on the total number of cells width and lengthwise. The voltage and energy targets, given by the vehicle optimizer, were equality constraints relaxed by surplus and slack variables (SV_V, SV_E). Finally, constraints were imposed on a minimum discharge and charge power of the accumulator such that the vehicle would be able produce the maximum discharge power set by the rules and be able to charge at the power set by the vehicle optimizer.

As mentioned in Section 3.3.2, the categorical cell type variable affected various charac-

teristics of the accumulator. This considerably increased the complexity of the design space. In addition, the other variables for this subsystem were ordinal. Typically, both these type of variables are difficult to handle for certain optimization algorithms as the neighborhood around a given value is unknown to the optimizer. Fortunately, the neighborhoods for these types of variables could be explicitly described within the MADS algorithm. This feature of the MADS was necessary in the successful optimization of this subsystem.

That being said, the accumulator optimization problem is

$$
\begin{aligned}
\min_{\mathbf{x}_{Acc}} \quad & -E_d(\mathbf{x}_{Acc}) \\
\text{s.t.} \quad & L_A(\mathbf{x}_{Acc}) - 24 \leq 0 \\
& W_A(\mathbf{x}_{Acc}) - 15 \leq 0 \\
& H_A(\mathbf{x}_{Acc}) - 9 \leq 0 \\
& V_A(\mathbf{x}_{Acc}) - (V_T + SV_V) \leq 0 \\
& -V_A(\mathbf{x}_{Acc}) + (V_T - SV_V) \leq 0 \\
& E_A(\mathbf{x}_{Acc}) - (E_T + SV_E) \leq 0 \\
& -E_A(\mathbf{x}_{Acc}) + (E_T - SV_E) \leq 0 \\
& -P_{discharge}(\mathbf{x}_{Acc}) + 80000 \leq 0 \\
& -P_{charge}(\mathbf{x}_{Acc}) + P_{charge_{min}} \leq 0 \\
& n_{C_{MW}} * n_{MW} - 36 \leq 0 \\
& -n_{C_{MW}} * n_{MW} + 6 \leq 0 \\
& n_{C_{ML}} * n_{ML} - 48 \leq 0 \\
& -n_{C_{ML}} * n_{ML} + 6 \leq 0 \\
& 1 \leq n_{C_{MW}} \leq 24 \\
& 1 \leq n_{C_{ML}} \leq 24 \\
& 1 \leq n_{MW} \leq 6 \\
& 1 \leq n_{ML} \leq 6 \\
& 2 \leq n_{C_P} \leq 6
\end{aligned}
\tag{4.6}
$$

with

$$\mathbf{x}_{Acc} = [T_C, n_{C_P}, n_{C_{MW}}, n_{C_{ML}}, n_{MW}, n_{ML}] \tag{4.7}$$

$$T_C \in \{TP6000, TP6200, TP6600, TP6800, ME6550\} \tag{4.8}$$

$$SV_V = 15 \tag{4.9}$$

$$SV_E = 100 \tag{4.10}$$

4.2.2 Gear train

The purpose of optimizing the gear train was to find the lightest possible design for a given gear ratio. To investigate the possibility of having different pairs of gear trains for the front and rear motors, the optimization of this subsystem was done twice. That is, the front and rear gear trains were treated as separate yet identical subsystems. The vehicle level optimizer provided a gear ratio target that was used by the gear train optimizer to find a lightweight design which met this set target, had the bending and surface durability to withstand a whole season of racing, met the geometric constraints and followed gear design best practices. More specifically, the gear ratio target was an equality constraint that was relaxed with equal surplus and slack variables (SV_{G}). As a result of limited space, the entire gear train needed to have a outer diameter smaller than or equal to 5.5 inches. The remaining constraints guided the optimizer into finding a reduction gear train and assured that the diametral pitches are within the best practice norms of spur gear design [18].

The mathematical formulation of the problem described above is

$$
\begin{aligned}
\min_{\mathbf{x}_{Gear}} \quad & m_{gear}(\mathbf{x}_{Gear}) \\
\text{s.t.} \quad & D_{CB_i}(\mathbf{x}_{Gear}) - 100 \leq 0 \\
& D_{CS_i}(\mathbf{x}_{Gear}) - 100 \leq 0 \\
& GR(\mathbf{x}_{Gear}) - (GR_T + SV_G) \leq 0 \\
& -GR(\mathbf{x}_{Gear}) + (GR_T - SV_G) \leq 0 \\
& n_{T_1} - n_{T_2} \leq 0 \\
& n_{T_3} - n_{T_2} \leq 0 \\
& n_{T_1} - n_{T_4} \leq 0 \\
& d_o(\mathbf{x}_{Gear}) - 5.5 \leq 0 \\
& -F_{W_1} + \frac{8}{DP_1} \leq 0 \\
& -F_{W_2} + \frac{8}{DP_2} \leq 0 \\
& F_{W_1} - 2\frac{n_{T_1}}{DP_1} \leq 0 \\
& F_{W_1} - 2\frac{n_{T_2}}{DP_1} \leq 0 \\
& F_{W_2} - 2\frac{n_{T_3}}{DP_2} \leq 0 \\
& F_{W_2} - 2\frac{n_{T_4}}{DP_2} \leq 0 \\
& 0 \leq F_{W_i} \leq 1.5 \\
& 18 \leq n_{T_i} \leq 120
\end{aligned}
\tag{4.11}
$$

with

$$\mathbf{x}_{Gear} = [DP_1, DP_2, n_{T_1}, n_{T_2}, n_{T_3}, n_{T_4}, F_{W_1}, F_{W_2}, O_{RG}] \tag{4.12}$$

$$D_i \in \{18, 20, 24, 28, 32\} \tag{4.13}$$

$$O_{RG} \in \{False, True\} \tag{4.14}$$

$$Feasible = \frac{n_{T_1}}{DP_1} + \frac{n_{T_2}}{DP_1} + \frac{n_{T_3}}{DP_2} == \frac{n_{T_4}}{DP_2} \tag{4.15}$$

$$SV_G = 0.5 \tag{4.16}$$

The MADS algorithm and its ability to describe the neighborhoods of variables was necessary to optimize the gear trains as all but the face width variables were either categorical or ordinal. In addition to this, the MADS optimizer was needed to handle the possibility of infeasible gear train designs if the gears were determine not to mesh together.

Chapter 5

Numerical Results

In order to determine the effectiveness of the the developed framework and identify how the different events affect the design of the vehicle, the above optimization framework was used to find the optimal vehicle for each of the five different events and the vehicle which maximizes the overall points across all events.

To properly compare the optimization results obtained, the latest fully developed vehicle by MFE was used as a baseline. This baseline vehicle and its subsystems are described in Tables 5.1, 5.2 and 5.3. As MFE did not use the MDO framework to conceive the baseline vehicle, the target variables (GR_{F_T}, GR_{R_T}, $P_{charge_{min}}$, E_T) were omitted from Table 5.1. These variables were only used in the coordination between the system and subsystem level optimizers. Tables 5.2 and 5.3 also show certain subsystem model outputs needed to interpret the optimization results.

Table 5.1: Baseline vehicle.

$\mathbf{GR_{F_T}}$	$\mathbf{GR_{R_T}}$	$\mathbf{P_{charge_{min}}}$ (W)	$\mathbf{E_T}$ (Wh)	$\boldsymbol{\alpha_{F3}}$ (deg)	$\boldsymbol{\alpha_{R2}}$ (deg)	$\boldsymbol{\alpha_{R3}}$ (deg)	$\mathbf{P_{limit}}$ (W)
NA	NA	NA	NA	0	0	0	74 000

Table 5.2: Baseline front and rear gear train designs.

Inputs									Outputs	
DP_1	DP_2	N_{T_1}	N_{T_2}	N_{T_3}	N_{T_4}	F_{W_1}	F_{W_2}	O_{RG}	GR	m_{gear} (kg)
18	18	18	53	19	90	0.45	1.2	1	13.95	4.87

Table 5.3: Baseline accumulator design.

Inputs						Outputs				
T_C	n_{C_P}	$n_{C_{MW}}$	$n_{C_{ML}}$	n_{MW}	n_{ML}	E_d (Wh/in^3)	$P_{discharge}$ (W)	P_{charge} (W)	E_A (Wh)	m_A (kg)
TP6000	2	3	8	2	3	3.51	181 440	31 968	6 394	48.52

Prior to launching the multidisciplinary design optimization study, the effects of the target variables given by the system optimizer on the accumulator subsystem were evaluated. More specifically, a full factorial sweep of different minimum charge powers and energy targets, with a fixed voltage target of 600 V, was done. For each of the different target combinations, an accumulator subsystem optimization was attempted. It was found that this subsystem was severally over constrained. With the voltage target parameter set at 600V, there were only two feasible accumulator designs. These are shown in Table 5.4 with design 2 being identical to the baseline design. Through the analysis of the best infeasible designs produced during the sweep, the voltage target and geometric constraints were determined to be the cause as one or both could not be satisfied while also satisfying the energy target constraint. Unfortunately, due to the lack of data surrounding the motor characteristics at other operating voltages, this constraint could not be relaxed. Similarly, the limited amount of space available in the chassis prevents the relaxation of the dimensional constraints. To deal with this reality, the MDO problem was solved twice using one of the feasible battery design as a parameter for each of the studies. This method was preferred to running the accumulator subsystem optimization within the MDO structure as it saved considerable amount of computational cost without changing the optimization results.

Table 5.4: Feasible accumulator designs at 600V.

	Inputs						Outputs				
Feasible Design	$\mathbf{T_C}$	$\mathbf{n_{C_P}}$	$\mathbf{n_{C_{MW}}}$	$\mathbf{n_{C_{ML}}}$	$\mathbf{n_{MW}}$	$\mathbf{n_{ML}}$	$\mathbf{E_d}$ (Wh/in^3)	$\mathbf{P_{discharge}}$ (W)	$\mathbf{P_{charge}}$ (W)	$\mathbf{E_A}$ (Wh)	$\mathbf{m_A}$ (kg)
1	TP6000	2	7	5	1	4	3.51	176 400	31 080	6 216	47.17
2	TP6000	2	3	8	2	3	3.51	181 440	31 968	6 394	48.52

Nonetheless, simply for academic purposes, an optimization study considering all events was done with relaxed accumulator voltage and geometric constraints.

That being said, this chapter will cover the analysis of the results obtained in the individual event optimization problems, the complete competition optimization study with the exact constraints imposed by MFE and the relaxed constraints detailed above.

5.1 Individual event optimization

By simply glancing at Tables 5.5, 5.6, 5.7 and 5.8, one can observe that the vehicle design is heavily dependent on the event. To this point, these tables will be used to interpret the results for each of the event specific optimization discussed in this section. The results of the optimization studies done on each of the FSAE competition events are shown in Table 5.5 with the best results highlighted in blue. Tables 5.6 and 5.7 show the optimal values for the vehicle and gear train variables for the highlight design. Finally, Table 5.8 presents a comparison between the lap simulation outputs produced by the baseline and optimal vehicle designs for each event.

Table 5.5: Individual event optimization results with best results shown in blue.

Event	Baseline	Optimal w/ Battery 1	Optimal w/ Battery 2
Acceleration	79.47	82.53	82.12
Skid-pad	59.93	61.77	61.55
Autocross	113.16	115.39	115.05
Endurance	255.85	258.43	260.14
Efficiency	84.45	97.91	97.99

Table 5.6: Optimal vehicle variables for each individual event optimization study.

	$\mathbf{GR_{F_T}}$	$\mathbf{GR_{R_T}}$	$\boldsymbol{\alpha_{F3}}$ (deg)	$\boldsymbol{\alpha_{R2}}$ (deg)	$\boldsymbol{\alpha_{R3}}$ (deg)	$\mathbf{P_{limit}}$ (W)
Acceleration	13.14	13.16	4	-4	-4	80 000
Skid-pad	5.52	6.36	-2.26	4	-3	80 000
Autocross	14.45	14.45	-4	4	-4	80 000
Endurance	13.89	13.87	-4	4	-4	74 785
Efficiency	14.22	14.10	4	-4	-4	10 000

Table 5.7: Optimal gear train variables for each individual event optimization study.

		Inputs									**Outputs**	
Event	**GT**	$\mathbf{DP_1}$	$\mathbf{DP_2}$	$\mathbf{N_{T_1}}$	$\mathbf{N_{T_2}}$	$\mathbf{N_{T_3}}$	$\mathbf{N_{T_4}}$	$\mathbf{F_{W_1}}$	$\mathbf{F_{W_2}}$	$\mathbf{O_{RG}}$	**GR**	$\mathbf{m_{gear}}$ (kg)
Acceleration	**Front**	24	24	21	51	18	90	0.33	0.52	0	13.14	1.57
	Rear	24	24	21	51	18	90	0.33	0.52	0	13.14	1.57
Skid-pad	**Front**	32	32	21	30	18	69	0.36	0.58	1	5.48	0.52
	Rear	32	32	25	36	18	79	0.28	0.59	1	6.32	0.57
Autocross	**Front**	24	24	21	54	18	93	0.33	0.55	0	14.29	1.74
	Rear	24	24	21	54	18	93	0.33	0.55	0	14.29	1.74
Endurance	**Front**	24	24	18	52	20	90	0.33	0.54	0	14	1.67
	Rear	24	24	18	52	20	90	0.33	0.54	0	14	1.67
Efficiency	**Front**	24	24	21	54	18	93	0.33	0.55	0	14.29	1.74
	Rear	24	24	18	52	20	90	0.33	0.54	0	14	1.67

Table 5.8: Lap simulation analysis for each individual event optimization study.

Event	Design	DF[1] (N)	DR[1] (N)	Max Speed (km/h)	Theoretical Max Speed (km/h)	Battery Mass (kg)	Total Unsprung Mass (kg)
Acceleration	**Baseline**	2 383.87	869.53	109.85	109.85	48.52	60.69
	Optimal	2 359.04	839.88	116.57	116.57	47.17	54.10
Skid-pad	**Baseline**	319.72	122.24	41.80	109.85	48.52	60.69
	Optimal	323.94	125.21	42.01	137.80	47.17	52.05
Autocross	**Baseline**	2 321.54	847.55	108.48	109.85	48.52	60.69
	Optimal	2 351.78	866.87	107.21	107.24	47.17	54.43
Endurance	**Baseline**	2 383.87	869.53	109.85	109.85	48.52	60.69
	Optimal	2 414.84	889.32	109.43	109.43	48.52	54.29
Efficiency	**Baseline**	2 383.87	869.53	109.85	109.85	48.52	60.69
	Optimal	2 359.04	839.88	67.73	68.48	48.52	54.36

5.1.1 Optimizing for acceleration

For the acceleration event, the optimizer found that the best result, shown in Table 5.5, is obtained when the vehicle is equipped with the lightest of the two battery options, has a lower gear ratio for higher top speed and has a low drag aerodynamic configuration. This was expected as the vehicle would not need a large battery pack as the energy consumption during the event is fairly low and it would not need much downforce aside for when it is traction limited at the very start of the event. That being said, the optimal design was estimated to produce 3.41% less drag while only reducing downforce by about 1.04% at the baseline maximum speed. In addition, the total weight reductions were about 7.94 kg, where 6.58kg are from the new gear train designs. These changes result in a score increase of 3.85%.

As Figure 5.1 and Table 5.8 demonstrate, both the baseline and optimal vehicles reach

[1]Measured at the baseline max speed with neutral vehicle attitude

their top speed during the acceleration event. Although the framework's final design has a higher maximum speed, both vehicles were limited by the 20 000 RPM limit of the motors. Thus, the increase in maximum speed was entirely a consequence of the lower gear ratio of the design. This result seems to indicate that the optimizer determined that further reductions in the gear ratio to increase the top speed would undermine the vehicle's acceleration capabilities sufficiently to negatively impact the results. Reducing the gear trains for the front motors would also not result in any gain as the rear motors would still limit the top speed.

Although it is barely noticeable, for approximately the first 25 meters, the proposed design has a lower acceleration rate as it has less downforce and is thus more traction limited than the baseline. However, as the speed of the vehicle increases, the lower drag and weight of the vehicle gives it a slight edge in acceleration. Therefore, the optimal gear train allows the vehicle to take advantage of all the available traction at the start of the event while permitting the vehicle to reach the highest top speed possible.

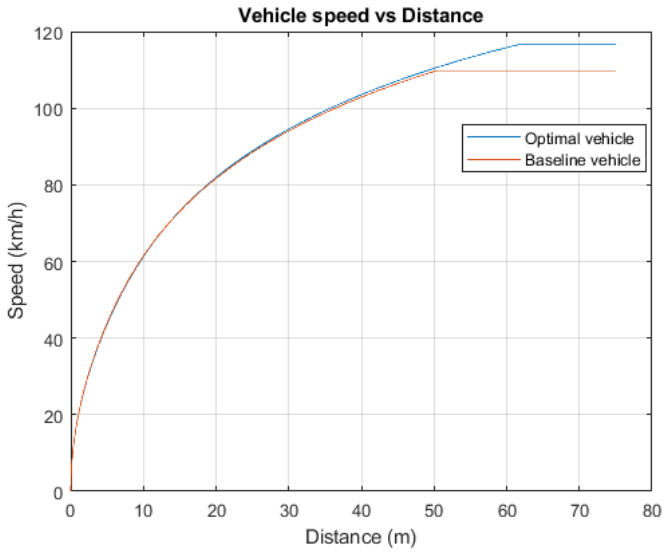

Figure 5.1: Speed differences of the optimal vehicle for the acceleration optimization study.

5.1.2 Optimizing for skid-pad

From the results in Table 5.5, the skid-pad optimized vehicle scores 3.07% higher than the baseline. Table 5.8, shows that this relatively larger increase in performance is due to the marginally larger top speed that the proposed vehicle can achieve. This increase in performance was obtained by using the lightest of the two battery options, a downforce biased aerodynamic configuration and light gear train designs. In more detail, the total mass was reduced by 9.99 kg, 8.64kg being a result of the new gear trains designs with the front assemblies being lighter. Comparing the downforce and drag at a speed of 41.80 km/h with no ride height deflection, the optimized design had 1.32% more downforce with 2.43% more drag.

From these results, it is fairly evident that the optimizer tried to minimize mass at all cost while also increasing the available traction by maximizing downforce. In fact, the lower gear ratio design of the front gear trains, with respect to the rear pair, was a result of the aggressive weight reduction. The optimizer found the gear ratio combination which would provide sufficient torque across all four wheels to maintain the maximum cornering speed while also reducing the mass to increase said maximum speed. This was possible as no motor is RPM-limited due to the low speeds of the skid-pad event.

5.1.3 Optimizing for autocross

From the results shown in Tables 5.5, 5.6, 5.7 and 5.8, it can be deduced that designing for the autocross event is centered around acceleration and high speed cornering. As this track has multiple corners of varying radii and a couple of slaloms, the vehicle is forced to repeatedly accelerate and decelerate. To reduce the time needed to traverse the track, and thus improve the score, the vehicle should maintain a higher speed around each corners and be able to accelerate at a higher rate after exiting corners. This can be achieved by increasing downforce, reducing the vehicle weight, and utilizing all of the traction that the tires can provide. As the tables demonstrate, the optimizer was able to do this by selecting a downforce

oriented aerodynamic setup, selecting the lightest accumulator available, reducing the mass of the gear trains and increasing the gear ratio to provide more torque at the contact patches. In fact, the downforce was improved by 1.30% with a drag increase of 2.28% and the total mass of the vehicle was reduced by 7.61 kg. As Figure 5.2 illustrates, the autocross optimal vehicle was able to achieve slightly higher cornering speeds on the high-speed corners and is able to accelerate at a higher rate on corner exits. These slight speed increases throughout the track resulted in a score improvement of 1.97%.

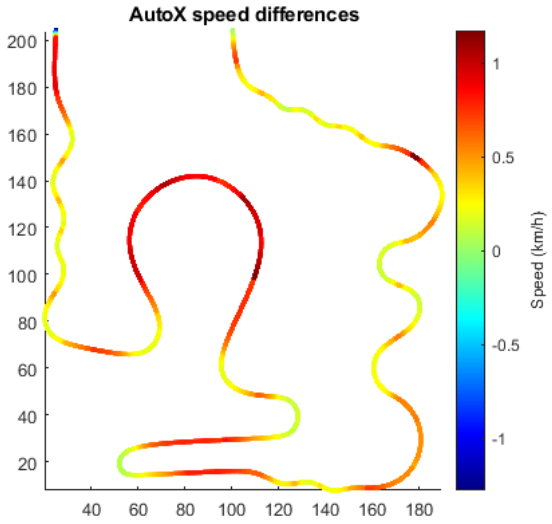

Figure 5.2: Speed differences of the optimal vehicle for the autocross optimization study.

5.1.4 Optimizing for endurance

When optimizing for only endurance points and completely disregarding the efficiency aspect of the event, the problem objective is comparable to the autocross optimization study. The main difference is the consideration of energy management in the MDO process due to the length of the race. For this reason, the power limit was considered a variable during this optimization study instead of being a parameter set at the 80 kW allowed by the rules. Looking at the results from Tables 5.5 and 5.6 and comparing them to the baseline values from 5.1, it can be observed that the optimal vehicle utilized the same higher capacity

accumulator design but was able to utilize an additional 4 785 W of power. That was possible while also keeping the same downforce oriented aerodynamic configuration found in the autocross optimization study. As indicated in Table 5.7, the only weight reductions achieved were from the lighter gear train designs.

Table 5.9: Energy related lap simulation results for the endurance optimization study.

Design	**Remaining Energy** (Wh)	**Total energy Used** (Wh)	**Total energy regenerated** (Wh)	**Drag**[2] **Losses** (Wh)
Baseline	1.28	10 156.50	3 764.18	2 383.53
Optimal	0.09	10 119.43	3 725.9	2 459.09

At first glance, it is difficult to determine where the 1.68% score improvement came from as the proposed design was able to draw more power, had more drag and had equal amounts of available energy. In fact, as Table 5.9 displays, both vehicles had little to no energy remaining in the accumulator. However, the table also demonstrates that the optimal design utilized less energy to complete the event. In other words, the new design was capable of utilizing the available energy more efficiently. Thus, despite the efficiency score not being considering in the optimization objective of this study, the optimizer still made the vehicle marginally more efficient. This was reflected in the efficiency scores achieved by the designs. The baseline vehicle had a score of 84.45 while the final proposed design had a score of 84.57, a 0.14% improvement. The need to improve the efficiency of the vehicle to increase performance is caused by the small and finite amount of available energy in the accumulator. As a matter of fact, the amount of energy is so restricted that both designs had over a third of all energy used during the event be regenerated. From this, it can be argued that efficiency would play a role in this particular optimization problem until the power limit can be increased to the 80 kW permitted by the rules.

[2]Measured over the entire event

This higher efficiency of the vehicle can be visualized in Figure 5.3. These images show that the proposed vehicle achieved the same or higher speeds in all areas with exception for the longer straights. Therefore, the improved higher downforce design enhances the preservation of the kinetic energy of the vehicle by allowing it to shorten braking distances and corner faster. Despite these shorter braking periods, Table 5.9 reveals that energy recuperation was barely affected. The lighter design also reduces the amount of energy required to accelerate. Over the course of 16 laps, these small efficiency gains provided the sufficient energy to expand the available power which permitted the proposed vehicle to accelerate out of the corners at a slightly higher rate.

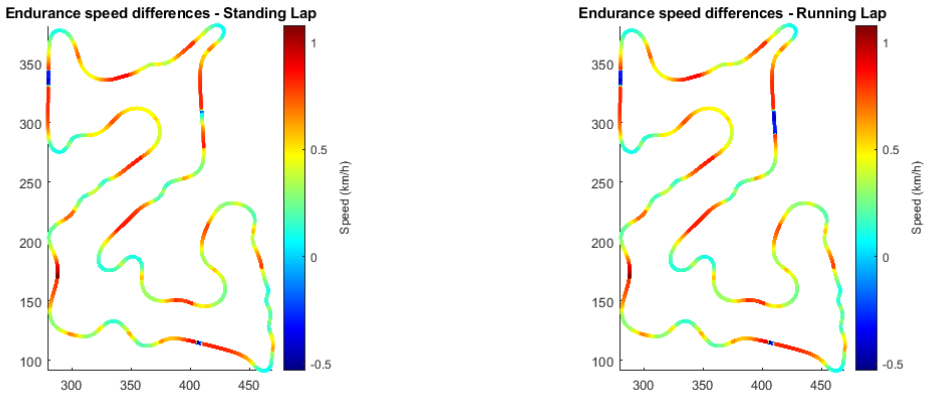

(a) Standing lap

(b) Running lap

Figure 5.3: Speed differences of the optimal vehicle for the endurance optimization study.

5.1.5 Optimizing for efficiency

The optimal values for the vehicle and subsystem variables in Tables 5.5, 5.6 and 5.7 indicate that utilizing the efficiency score as the optimization objective produces the most distinct vehicle out of all the individual event optimization studies. This is unsurprising since the efficiency scoring method is exceedingly sensitive to the average energy use per lap, as is illustrated in Figure 3.5. In contrast to the other individual event optimization problems, the optimizer completely disregarded lap time as an objective for this study and solely focused on minimizing the average energy expended per lap after accounting for regenerated

energy. As a matter of fact, the average lap time of the most efficient vehicle is 98.17 seconds compared to the 81.10 seconds of the baseline vehicle. If it was not for the lower 10 kW bound arbitrarily imposed on the power limit, the optimizer would have undoubtedly continued to reduce the power limit until the average lap time matched the threshold $t_{avg_{max}}$ of 114.80 given by Equation (3.6). The optimizer remarkably improved the efficiency score by 16%. However, the associated endurance score dropped to 119.13 or by 53.44% .

Table 5.10: Energy related lap simulation results for the efficiency optimization study.

Design	**Remaining Energy** (Wh)	**Total energy Used** (Wh)	**Total energy regenerated** (Wh)	**Drag**[3] **Losses** (Wh)
Baseline	1.28	10 156.50	3 764.18	2 383.53
Optimal	4 081.35	3 638.82	1 326.58	1 334.97

As alluded to previously, most of the efficiency gains were obtained by significantly lowering the power limit of the vehicle which severely crippled the speed of the vehicle. This is clearly displayed in Figure 5.4. Interestingly, the front gear ratio was increased, relative to the rear gear train, to seemingly take advantage of the fact that the front tires are loaded under braking. This increased the regenerated energy under braking. The same aerodynamic setup from the acceleration optimization study was chosen for its lower drag. Lastly, the accumulator with the highest capacity was chosen. As shown in Table 5.10, this results in the vehicle being capable of ending the endurance race with 4 081.35 Wh of energy or 63.83% of the energy it started with.

[3]Measured over the entire event

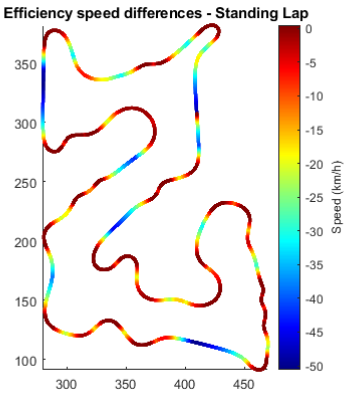

(a) Standing lap

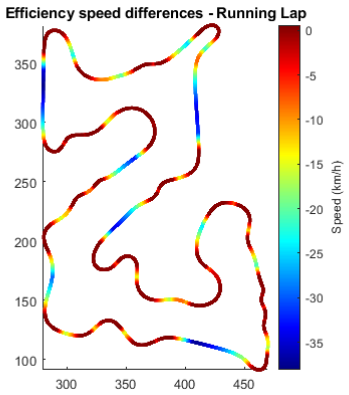

(b) Running lap

Figure 5.4: Speed differences of the optimal vehicle for the efficiency optimization study.

5.2 Optimizing for all events

Given that the endurance score represents 275 points of the total 675 points available, it was no surprise that the best overall vehicle resembled the endurance optimal design. Comparing the design obtained via the the overall optimization study to those of the endurance optimization confirm that the designs are completely identical.

Even though the overall optima would be considered suboptimal for the other event specific optimization studies, the lower weight from the gear trains and higher downforce to drag ratio of this concept contributes to small gains across all events when compared to the baseline. As shown in Table 5.11, the total score difference is 5.4 which is an increase of only 0.9%. Although this improvement may seem small, it is very important to note that the baseline vehicle was the final design produced by MFE over 2 years of continuous design iteration. The ultimate purpose of this MDO framework is to explore the design space during the conceptual design phase. The fact that the methodology in this work found an improvement on a mature design is a clear indication of its capabilities.

Table 5.11: All event optimization results with best result shown in blue.

Design	**Accel. Score**	**Skid-Pad Score**	**Autocross Score**	**Endurance Score**	**Efficiency Score**	**Total Score**
Baseline	79.47	59.93	113.16	255.85	84.45	595.87
Optimal w/ Battery 1	80.61	61.42	115.37	257.62	85.16	600.18
Optimal w/ Battery 2	80.34	61.21	115.01	260.14	84.57	601.27

Table 5.12: Optimal vehicle variables for the overall competition optimization study.

$\mathbf{GR_{F_T}}$	$\mathbf{GR_{R_T}}$	$\mathbf{P_{charge_{min}}}$ (W)	$\mathbf{E_T}$ (Wh)	$\boldsymbol{\alpha_{F3}}$ (deg)	$\boldsymbol{\alpha_{R2}}$ (deg)	$\boldsymbol{\alpha_{R3}}$ (deg)	$\mathbf{P_{limit}}$ (W)
13.97	14.05	NA	NA	-4	4	-4	74 756

Table 5.13: Front and rear gear train designs for the overall competition optimization study.

Inputs									**Outputs**	
$\mathbf{DP_1}$	$\mathbf{DP_2}$	$\mathbf{N_{T_1}}$	$\mathbf{N_{T_2}}$	$\mathbf{N_{T_3}}$	$\mathbf{N_{T_4}}$	$\mathbf{F_{W_1}}$	$\mathbf{F_{W_2}}$	$\mathbf{O_{RG}}$	**GR**	$\mathbf{m_{gear}}$ (kg)
24	24	18	52	20	90	0.33	0.54	0	14	1.67

5.3 Optimizing for all events with relaxed constraints

Assuming that the motor characteristics would remain unchanged at different operating voltages, the surplus and slack constraints around the voltage target were relaxed to ± 100V and the maximum length and width constraints were increased by 20%. Although these constraints were relaxed, a full factorial sweep of the new design space yielded only 20 unique battery pack designs. This made finding these feasible concepts within the design space

difficult for the optimizer which resulted in exceptionally long execution times. To accelerate the process, 20 separate optimization studies were done with each of the accumulator designs shown in Table 5.14.

The results of the 20 MDO studies with relaxed constraints demonstrate the impact of the different accumulator properties on the overall performance of the vehicle. Looking at only the results of the top 10 vehicle designs in Tables 5.15 and 5.16, it can be observed that the accumulator design can have an effect on the design choices of the other subsystems. In addition, the results indicate that there is a trade-off between accumulator mass, regenerative capability and capacity. More precisely, the benefits of increasing the available energy or regenerative capability can be undone if the accumulator mass is also increased significantly. This demonstrates the importance of including this subsystem within an MDO framework.

Table 5.14: Accumulator designs with relaxed constraints.

	Inputs						Outputs				
Relaxed Design	$\mathbf{T_C}$	$\mathbf{n_{C_P}}$	$\mathbf{n_{C_{MW}}}$	$\mathbf{n_{C_{ML}}}$	$\mathbf{n_{MW}}$	$\mathbf{n_{ML}}$	$\mathbf{E_d}$ (Wh/in^3)	$\mathbf{V_A}$ (V)	$\mathbf{P_{charge}}$ (W)	$\mathbf{E_A}$ (Wh)	$\mathbf{m_A}$ (kg)
1	ME6550	2	3	5	2	5	3.71	630	14 541	7 271	51.95
2	ME6550	2	4	4	2	4	3.70	538	12 408	6 204	44.33
3	ME6550	2	4	5	2	4	3.75	672	15 510	7 755	55.41
4	ME6550	2	6	11	1	2	3.89	554	12 796	6 398	45.72
5	ME6550	2	8	5	1	3	3.79	504	11 633	5 816	41.56
6	ME6550	2	8	9	1	2	3.89	605	13 959	6 980	49.87
7	TP6000	2	3	5	2	5	3.43	630	33 300	6 660	50.54
8	TP6000	2	4	4	2	4	3.41	538	28 416	5 683	43.13
9	TP6000	2	4	5	2	4	3.47	672	35 520	7 104	53.91
10	TP6000	2	6	11	1	2	3.61	554	29304	5 861	44.47
11	TP6000	2	8	9	1	2	3.61	605	31 968	6 394	48.52
12	TP6000	3	8	5	1	3	3.77	504	39 960	7 992	60.65
13	TP6600	2	4	4	2	4	2.81	538	75 018	6 252	56.45
14	TP6600	2	4	5	2	4	2.85	672	93 773	7 814	70.56
15	TP6600	2	4	6	2	3	2.87	605	84 396	7 033	63.51
16	TP6600	2	7	5	1	4	2.87	588	82051	6 838	61.74
17	TP6600	2	7	7	1	3	2.91	617	86 154	7 179	64.83
18	TP6600	2	8	5	1	3	2.88	504	70 330	5 861	52.92
19	TP6800	2	4	5	2	4	3.09	672	40 256	8 051	65.23
20	TP6800	2	8	5	1	3	3.12	504	30 192	6 038	48.92

Table 5.15: Top 10 all event optimization results with relaxed battery constraints.

Design	Accel. Score	Skid-Pad Score	Autocross Score	Endurance Score	Efficiency Score	Total Score
Optimal w/ Battery 18	80.35	60.49	113.79	259.74	92.05	606.43
Optimal w/ Battery 13	79.43	59.93	112.89	257.78	92.70	602.73
Optimal w/ Battery 11	80.34	61.19	115.01	260.12	84.58	601.24
Optimal w/ Battery 7	79.93	60.88	114.50	260.86	84.37	600.54
Optimal w/ Battery 10	82.86	61.90	115.87	250.82	86.31	597.76
Optimal w/ Battery 16	77.98	59.12	111.58	254.91	93.54	597.12
Optimal w/ Battery 9	79.25	60.34	113.65	259.01	84.84	597.09
Optimal w/ Battery 15	77.50	58.85	111.14	253.96	93.8	595.26
Optimal w/ Battery 20	80.26	61.13	114.91	252.77	85.70	594.76
Optimal w/ Battery 17	77.16	58.64	110.8	253.24	94.00	593.84

Table 5.16: Optimal vehicle variables for the top 10 overall competition optimization studies with relaxed constraints.

Design	$\mathbf{GR_{F_T}}$	$\mathbf{GR_{R_T}}$	$\mathbf{P_{charge_{min}}}$ (W)	$\mathbf{E_T}$ (Wh)	$\boldsymbol{\alpha_{F3}}$ (deg)	$\boldsymbol{\alpha_{R2}}$ (deg)	$\boldsymbol{\alpha_{R3}}$ (deg)	$\mathbf{P_{limit}}$ (W)
Optimal w/ Battery 18	13.65	13.79	NA	NA	-4	3.93	-4	80 000
Optimal w/ Battery 13	13.64	13.85	NA	NA	-3.90	3.96	-4	80 000
Optimal w/ Battery 11	13.97	14.05	NA	NA	-4	4	-4	74 756
Optimal w/ Battery 7	14.00	14.05	NA	NA	-4	4	-4	80 0006
Optimal w/ Battery 10	13.28	13.15	NA	NA	-4	3.90	-4	55 349
Optimal w/ Battery 16	13.68	13.80	NA	NA	-3.94	4	-4	80 000
Optimal w/ Battery 9	14.00	14.05	NA	NA	-4	4	-4	80 000
Optimal w/ Battery 15	13.68	13.80	NA	NA	-3.97	3.94	-4	80 000
Optimal w/ Battery 20	14.00	14.05	NA	NA	-3.98	4	-4	60 956
Optimal w/ Battery 17	13.68	13.80	NA	NA	-3.91	3.71	-4	80 000

Chapter 6

Conclusion

A distributed multidisciplinary design optimization framework was developed for use in the conceptual design phase of vehicles from McGill Formula Electric. This work focuses on the optimization of an electric vehicle, competing in multiple events, considering three distinct subsystems: the external aerodynamics, the battery pack and the front and rear gear trains. While the model for the gear train was provided by MFE, models for the other two subsystems were developed specifically for this work. Moreover, a new lap simulation method to evaluate and analyze the various concepts was created. Existing tire and motor models were used to improve the accuracy of this lap simulation method. The objective of the optimization problem of this work was to find the vehicle which maximizes the overall points in the FSAE competition. To accomplish this, the various event scoring functions were combined into a single objective.

In all optimization studies, the proposed conceptual design methodology was shown to improve on the very mature design of the benchmark vehicle. Besides providing an excellent initial concept, the framework provides extensive amounts of data that can be used to highlight where the improvements were made and what areas need additional design work.

The optimization studies also underscored a few deficiencies in MFE's latest vehicle which was used as a baseline for this work. These issues include a needlessly heavy gear train design

and over constraint accumulator design. Another potentially issue is the active boundary constraints for the aerodynamic related variables which may be an indication of a poorly design aerodynamic package.

Furthermore, the results indicate that considering the various different events in the optimization objective is unnecessary for FSAE applications. This is due to the fact that the competition is heavily weighted towards the endurance event. Moreover, the findings from the individual event optimization studies denotes a potential new use for this framework. The FSAE rules allow for certain parts of the vehicle, such as the angle of attack of the aerodynamic elements, to be changed in-between events. Identifying these different areas that can be altered and optimizing them for each event could improve the overall performance of the vehicle. Therefore, the developed framework can be used as a tool to generate designs in the conceptual design phase and as a tool to setup the vehicle for each event.

Lastly, the capabilities of the framework to consider energy usage and optimize for efficiency was also demonstrated. Based on the literature review of automotive related optimization, this appears to be a novel contribution to the field of automotive multidisciplinary design optimization.

6.1 Outlook

Although this work demonstrated the benefit of utilizing MDO methods in the conceptual design process of electric FSAE vehicles, the framework lacked coupling between the evaluated subsystems and is currently only capable of identifying high-order interactions between components. Adding new subsystems could link existing subsystems. An example of such a system would be the motor cooling which would add links between the external aerodynamics and accumulator subsystems. This would contribute to a more meaningful multidisciplinary design optimization and analysis. Besides adding new subsystems, additional improvements to the framework can be in the form of refinements to the models used. For example, a

higher degree of freedom aerodynamic model, which also considers steering angle, roll and yaw, could capture new interactions that are presently disregarded. A new motor model that accounts for various voltages would increase the amount of feasible accumulator designs and facilitate the exploration of the accumulator design space by the optimizer. Improving the lap simulations to include transient behaviour would enable the evaluation of new variables at the vehicle level such as suspension stiffness and dampening. Another potential way to build on the lap simulations would be to consider vehicle displacements along the width of the track and adding a driver model, which optimizes driver inputs (steering, throttle and braking), to find the best racing line. However, it is important to note that [19] claims that drivers struggle to follow an optimal path to $\pm$ 1 m while at racing speeds. Taking into account that the width of FSAE tracks can be a little as 3.5 m and MFE's vehicle has track width of about 1.1 m, the vehicle would only be able to travel approximately $\pm$ 1 m widthwise from the centerline. Whether the claims of [19] hold true for the low speeds and the low driver caliber is to be determined.

Moreover, little to no attention was given to setting the correct optimizer parameters. Therefore, both the results and execution times could potentially be improved by exploring new optimizer settings. In fact, the total execution times for the optimization studies covered were approximately three core-hours on a Ryzen 3700X processor. This highlights another area of potential improvement. Future work by MFE to improve computational efficiency could include refactoring the code, improving task parallelism and comparing alternative MADS implementations.

Finally, the use of a single objective function for this work was done because the rules of FSAE competitions weight the each event differently. However, this is not the case in other motorsports championships, such as Formula One, where each race is considered equal. Thus, the multi-objective nature of winning a championship can be viewed differently. In these type of competitions, Pareto fronts can be used to identify multiple designs which equally maximize the overall competition points. This enables teams to selectively favour certain

designs based of a number of factors, even non-engineering related ones. For example, Ferrari can select a design on the Pareto front which would score better in their home race without compromising the entire championship. As such, a similar project to the one presented in this work could be conceived to explore the optimization of vehicles destined to compete in motorsports championship with equally weighted events.

Bibliography

[1] "2021 Formula SAE Rules," last accessed on 2021-06-10. [Online]. Available: https://www.fsaeonline.com/cdsweb/gen/DocumentResources.aspx

[2] F. Altun, S. A. Tekin, S. Gürel, and M. Cernat, "Design and optimization of electric cars. a review of technological advances," in *2019 8th International Conference on Renewable Energy Research and Applications (ICRERA)*, 2019, pp. 645–650.

[3] J. R. R. A. Martins and A. B. Lambe, "Multidisciplinary design optimization: A survey of architectures," *AIAA Journal*, vol. 51, no. 9, pp. 2049 – 2075, 2013. [Online]. Available: http://dx.doi.org/10.2514/1.J051895

[4] R. Bäckryd, A.-B. Ryberg, and L. Nilsson, "Multidisciplinary design optimization methods for automotive structures," *International Journal of Automotive and Mechanical Engineering*, vol. 14, pp. 4050–4067, 03 2017.

[5] H. M. Kim, D. G. Rideout, P. Y. Papalambros, and J. L. Stein, "Analytical target cascading in automotive vehicle design," *Journal of Mechanical Design*, vol. 125, no. 3, pp. 481–489, 09 2003. [Online]. Available: https://doi.org/10.1115/1.1586308

[6] N. Kang, M. Kokkolaras, P. Y. Papalambros, S. Yoo, W. Na, J. Park, and D. Featherman, "Optimal design of commercial vehicle systems using analytical target cascading," *Structural and Multidisciplinary Optimization*, vol. 50, no. 6, pp. 1103–1114, Dec 2014.

[7] N. Kang, M. Kokkolaras, and P. Y. Papalambros, "Solving multiobjective optimization problems using quasi-separable MDO formulations and analytical target cascading," *Structural and Multidisciplinary Optimization*, vol. 50, no. 5, pp. 849–859, Nov 2014.

[8] J. Muñoz, G. Gutierrez, and A. Sanchis, "Multi-objective evolution for car setup optimization," in *2010 UK Workshop on Computational Intelligence (UKCI)*, 2010, pp. 1–5.

[9] M. Köle, A. S. Etaner-Uyar, B. Kiraz, and E. Özcan, "Heuristics for car setup optimisation in TORCS," in *2012 12th UK Workshop on Computational Intelligence (UKCI)*, 2012, pp. 1–8.

[10] C. McAllister, T. Simpson, K. Hacker, and K. Lewis, *Application of Multidisciplinary Design Optimization to Racecar Design and Analysis*. [Online]. Available: https://arc.aiaa.org/doi/abs/10.2514/6.2002-5608

[11] M. Fischer, M. Werber, and P. V. Schwartz, "Batteries: Higher energy density than gasoline?" *Energy Policy*, vol. 37, no. 7, pp. 2639 – 2641, 2009. [Online]. Available: http://www.sciencedirect.com/science/article/pii/S0301421509001323

[12] Huilong Yu, F. Castelli-Dezza, and F. Cheli, "Optimal powertrain design and control of a 2-IWD electric race car," in *2017 International Conference of Electrical and Electronic Technologies for Automotive*, 2017, pp. 1–7.

[13] H. Yu, F. Cheli, and F. Castelli-Dezza, "Optimal design and control of 4-IWD electric vehicles based on a 14-DOF vehicle model," *IEEE Transactions on Vehicular Technology*, vol. 67, no. 11, pp. 10 457–10 469, Nov 2018.

[14] "Awards & results - Formula SAE Electric," last accessed on 2021-06-10. [Online]. Available: https://www.sae.org/attend/student-events/formula-sae-electric/awards-results

[15] I. Besselink, A. Schmeitz, and H. Pacejka, "An improved magic formula/swift tire model that can handle inflation pressure changes," *Vehicle System Dynamics*, vol. 48, pp. 337 – 52, 2010//. [Online]. Available: http://dx.doi.org/10.1080/00423111003748088

[16] "FSAE TTC - Formula SAE Tire Testing Consortium," last accessed on 2021-06-10. [Online]. Available: https://www.calspan.com/services/transportation-testing-research-equipment/fsae-ttc/

[17] R. D'Souza, J. Patsavellas, and K. Salonitis, "Automated assembly of Li-ion vehicle batteries: A feasibility study," *Procedia CIRP*, vol. 93, pp. 131–136, 2020, 53rd CIRP Conference on Manufacturing Systems 2020. [Online]. Available: https://www.sciencedirect.com/science/article/pii/S2212827120307460

[18] R. L. Norton, *Chapter 12: Spur Gears*, 5th ed. Prentice Hall, 2014, p. 713–778.

[19] D. L. Brayshaw and M. F. Harrison, "A quasi steady state approach to race car lap simulation in order to understand the effects of racing line and centre of gravity location," *Proceedings of the Institution of Mechanical Engineers, Part D: Journal of Automobile Engineering*, vol. 219, no. 6, pp. 725–739, 2005. [Online]. Available: https://doi.org/10.1243/095440705X11211

[20] S. Le Digabel, "Algorithm 909: Nomad: Nonlinear optimization with the MADS algorithm," *ACM Trans. Math. Softw.*, vol. 37, no. 4, Feb. 2011. [Online]. Available: https://doi-org.proxy3.library.mcgill.ca/10.1145/1916461.1916468

[21] A. B. Lambe and J. R. R. A. Martins, "Extensions to the design structure matrix for the description of multidisciplinary design, analysis, and optimization processes," *Structural and Multidisciplinary Optimization*, vol. 46, pp. 273–284, 2012.